arXiv:0705.3182v1 [astro-ph] 22 May 2007

Gravitational instability in binary protoplanetary disks

Lucio Mayer[1] Alan Boss[2] and Andrew F. Nelson[3]

[1] Institute for Theoretical Physics, University of Zurich, and Institute for Astronomy, ETH Zurich, Zurich, Switzerland lucio@phys.ethz.ch
[2] Carnegie Institution of Washington, Washington, USA boss@dtm.ciw.edu
[3] Los Alamos National Laboratory, USA andy.nelson@lanl.gov

Summary. We review the models and results of simulations of self-gravitating, gaseous protoplanetary disks in binary star systems. These models have been calculated by three different groups with three different computational methods, two particle-based and one grid-based. We show that interactions with the companion star can affect the temperature distribution and structural evolution of disks, and discuss the implications for giant planet formation by gravitational instability as well as by core accretion. Complete consensus has not been reached yet on whether the formation of giant planets is promoted or suppressed by tidal interactions with a companion star. While systems with binary separations of order 100 AU or larger appear to behave more or less as in isolation, systems with smaller separations exhibit an increased or decreased susceptibility to fragmentation, depending on the details of thermodynamics, in particular on the inclusion or absence of artificial viscosity, and on the initial conditions. While code comparisons on identical problems need to be carried out (some of which are already in progress) to decide which computer models are more realistic, it is already clear that relatively close binary systems, with separations of order 60 AU or less, should provide strong constraints on how giant planets form in these systems.

1 Introduction

Gravitational instabilities (GIs) can occur in any region of a gas disk that becomes sufficiently cool or develops a high enough surface density. In the nonlinear regime, GIs can produce local and global spiral waves, self-gravitating turbulence, mass and angular momentum transport, and disk fragmentation into dense clumps and substructure. It has been quite some time since the idea was first suggested (Kuiper 1951; Cameron 1978) and revived by Boss (1997, 1998a) that the dense clumps in a disk fragmented by GIs may become self-gravitating precursors to gas giant planets. This particular idea for gas giant planet formation has come to be known as the *disk instability* theory. The idea is appealing since gravitational instability develops on very short

timescales compared to the accumulation of planetesimals by gravity and the subsequent accretion of gas by a rocky core, the conventional two-stage formation giant planet formation theory known as *core accretion* (see the chapter by Marzari et al.).

The particular emphasis of this review chapter is on how gravitational instability develops when a protoplanetary disk is not isolated but is a member of a binary or multiple star system (see the chapter by Prato & Weinberger). Indeed such a configuration is likely to be the most common in the Galaxy: the majority of solar-type stars in the Galaxy belong to double or multiple stellar systems (Duquennoy & Mayor 1991; Eggenberger et al. 2004). Radial velocity surveys have shown that planets exist in binary or multiple stellar systems where the stars have separations from ~ 20 to several thousand AU (Eggenberger et al. 2004; see the chapter by Eggenberger & Udry). Although the samples are still small, attempts have been made to compare properties of planets in single and multiple stellar systems (Patience et al. 2002; Udry et al. 2004). Adaptive optics surveys designed to quantify the relative frequency of planets in single and multiple systems are underway (Udry et al. 2004; Chauvin et al. 2006). At least 30% of extrasolar planetary systems appear to occur in binary or multiple star systems (Raghavan et al. 2006). These surveys could offer a new way to test theories of giant planet formation, provided that different formation models yield different predictions about the effects of a stellar companion.

1.1 Gravitational instabilities

The parameter that determines whether GIs occur in thin gas disks is

$$Q = c_s \kappa / \pi G \Sigma, \tag{1}$$

where c_s is the sound speed, κ is the epicyclic frequency at which a fluid element oscillates when perturbed from circular motion, G is the gravitational constant, and Σ is the surface density. In a nearly Keplerian disk, $\kappa \approx$ the rotational angular speed Ω. For axisymmetric (ring-like) disturbances, disks are stable when $Q > 1$ (Toomre 1964). At high Q-values, pressure, represented by c_s in (1), stabilizes short wavelengths, and rotation, represented by κ, stabilizes long wavelengths. The most unstable wavelength when $Q < 1$ is given by $\lambda_m \approx 2\pi^2 G\Sigma/\kappa^2$.

Modern numerical simulations, beginning with Papaloizou & Savonije (1991), show that nonaxisymmetric disturbances, which grow as multi-armed spirals, become unstable for $Q <\sim 1.5$. Because the instability is both linear and dynamic, small perturbations grow exponentially on the time scale of a rotation period $P_{rot} = 2\pi/\Omega$. The multi-arm spiral waves that grow have a predominantly trailing pattern, and several modes can appear simultaneously (Boss 1998a; Laughlin et al. 1997; Nelson et al. 1998; Pickett et al. 1998).

Numerical simulations show that, as GIs emerge from the linear regime, they may either saturate at nonlinear amplitude or grow enough to fragment

the disk. Two major effects control or limit the outcome – disk thermodynamics and nonlinear mode coupling. At this point, the disks also develop large surface distortions. As emphasized by Pickett et al. (1998, 2000, 2003), the vertical structure of the disk plays a crucial role, both for cooling and for essential aspects of the dynamics. As a result, except for isothermal disks, GIs tend to have large amplitudes at the surface of the disk.

Using second and third-order governing equations for spiral modes and comparing their results with a full nonlinear hydrodynamics treatment, Laughlin et al. 1998 studied nonlinear mode coupling in the most detail. Even if only a single mode initially emerges from the linear regime, power is quickly distributed over modes with a wide variety of wavelengths and number of arms, resulting in a self-gravitating turbulence that permeates the disk. In this *gravitoturbulence*, gravitational torques and even Reynold's stresses may be important over a wide range of scales (Nelson et al. 1998; Gammie 2001; Lodato & Rice 2004; Mejía et al. 2005).

As the spiral waves grow, they can steepen into shocks that produce strong localized heating (Pickett et al. 1998, 2000a; Nelson et al. 2000). Gas is also heated by compression and through net mass transport due to gravitational torques. The ultimate source of GI heating is work done by gravity. The subsequent evolution depends on whether a balance can be reached between heating and the loss of disk thermal energy by radiative or convective cooling. The notion of a balance of heating and cooling in the nonlinear regime was described as early as 1965 by Goldreich & Lynden-Bell and has been used as a basis for proposing α-treatments for GI-active disks (Paczyński 1978; Lin & Pringle 1987). For slow to moderate cooling rates, numerical experiments verify that thermal self-regulation of GIs can be achieved (Tomley et al. 1991; Pickett et al. 1998, 2000a, 2003; Nelson et al. 2000; Gammie 2001; Rice et al. 2003b; Lodato & Rice 2004, 2005; Mejía et al. 2005; Cai et al. 2006a,b). Q then hovers near the instability limit, and the nonlinear amplitude is controlled by the cooling rate. There have been various attempts to model radiative cooling in self-gravitating disks. For a recent overview of the different methods appearing in the literature and for a general discussion of gravitational instability in protoplanetary disks, we point the reader to Durisen et al. (2007). In this chapter we will focus on the radiative cooling models that have been used in the few existing works on binary self-gravitating protoplanetary disks.

1.2 Fragmentation and survival of clumps

As shown first by Gammie (2001) for local thin-disk calculations and later confirmed by Rice et al. (2003b) and Mejía et al. (2005) in full 3D hydro simulations, disks with a fixed cooling time, $t_{cool} = U/\dot{U}$, fragment for sufficiently fast cooling, specifically when $t_{cool} \leq 3\Omega^{-1}$, or, equivalently, $t_{cool} \leq P_{rot}/2$. Finite thickness has a slight stabilizing influence (Rice et al. 2003b; Mayer et al. 2004a). When dealing with realistic radiative cooling, however, one cannot apply this simple fragmentation criterion to arbitrary initial disk models.

One has to apply it to the asymptotic phase after nonlinear behavior is well-developed (Johnson & Gammie 2003). Cooling times can be much longer in the asymptotic state than they are initially (Cai et al. 2006a,b; Mejía et al., in preparation). For disks evolved under isothermal conditions, where a simple cooling time cannot be defined, local thin-disk calculations show fragmentation when $Q < 1.4$ (Johnson & Gammie 2003). This is roughly consistent with results from global simulations (e.g., Boss 2000; Nelson et al. 1998; Pickett et al. 2000a, 2003; Mayer et al. 2002, 2004a). Figure 1 shows a classic example of a fragmenting disk.

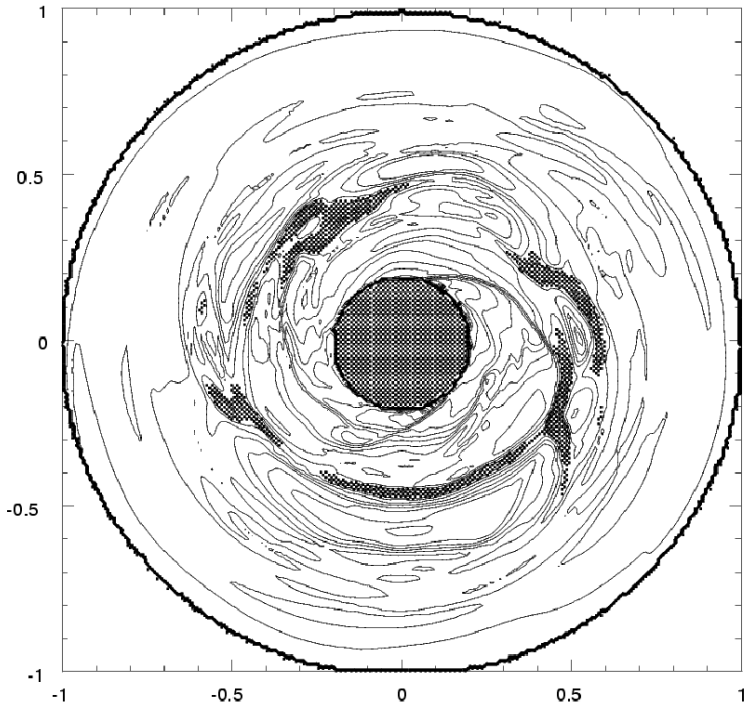

Fig. 1. Midplane density contours after 339 yr of evolution of a $0.091 M_{\odot}$ disk in orbit around a single $1 M_{\odot}$ protostar, showing the formation of a self-gravitating clump of mass $1.4 M_{Jup}$ at 4 o'clock (Boss 2001).

Rice et al. (2003b) also found that clumps could form in disks with even longer cooling times ($t_{cool} = 5\Omega^{-1}$) if the disk mass was increased. This latter estimate is in agreement with the time scales for cooling found in 3D models with diffusion approximation radiative transfer and convective-like motions that led to fragmentation into self-gravitating clumps (Boss 2001, 2004a).

Although there is general agreement on conditions for fragmentation, two important questions remain. Do real disks ever cool fast enough for fragmentation to occur, and do the fragments last long enough to contract into permanent protoplanets before being disrupted by tidal stresses, shear stresses, physical collisions, and shocks? Recent simulations have just begun to address the issue of the long term survival of clumps once they have been produced in a disk (Durisen et al. 2007). None of these long-term simulations has explored the case of binary systems and therefore their results are not necessarily valid in that case (for example they do not take into account the effect of eventual orbital resonances with the companion that might). . However, except for clumps forming at the very periphery of one of the two disks, one would expect the tidal stresses to be dominated by the central star of their own disk, in which case the results of isolated disks are still relevant. In addition, clumps are unlikely to form near the outskirts of disks since the surface density should be too low there. High spatial resolution appears to be crucial for the survival of clumps. Pickett et al. (2003) found that 256 azimuthal cells were not enough to resolve self-gravity on a scale of a fraction of AU, leading to artificial dissolution of overdensities. An increased ability of clumps to persist and become gravitationally bound as the resolution is increased was also found by Boss (2001) and Mayer et al. (2004). High spatial resolution of the gravitational force is crucial, as is the accuracy of a gravity solver for a given resolution element. These features are extremely code-dependent and are briefly discussed below in section 2.2.

2 Numerical Techniqes and Assumptions

To date, only three papers have been published that consider the possibility of forming giant planets by disk instability in binary star systems: Nelson (2000), Mayer et al. (2005), and Boss (2006b). In short, Nelson (2000) found that binarity prevented fragmentation from occurring, Boss (2006b) found that binarity could enhance clump formation, and Mayer et al. (2005) found the binarity could discourage fragmentation in some cases, but permit it in other cases. These three papers are the focus of the remainder of this chapter, as we try to decipher the reasons for this apparent dispersion in outcomes.

2.1 Hydrodynamics methods

Three codes have been used so far to follow the evolution of binary protoplanetary disks, two smoothed particle hydrodynamics (SPH) codes (Nelson 2000; Mayer et al. 2005) and one finite-difference grid-based code (Boss 2006b; described in detail by Boss & Myhill 1992). The two SPH codes are, respectively, a modified version (Nelson 2000) of a code originally developed by Benz (1990) and GASOLINE (Wadsley et al. 2004; Mayer et al. 2005). We begin with a description of the codes.

Although the two SPH codes are based on a very similar implementation of SPH, there are differences in some aspects that might be important for understanding differences in results. One major difference is that the version of the code used in Nelson (2000) is 2D while GASOLINE is 3D, as is the Boss (2006b) code. Evidence has been accumulated recently that gravitational instability in a protoplanetary disk is an intrinsically three-dimensional phenomenon (Cai et al. 2006a,b). At the same time, at the resolution for which affordable simulations can be done, 3D codes resolve only very poorly the structure of the disk in the third dimension. Nelson (2006) has shown that if the vertical structure is not well resolved, both from a hydrodynamical standpoint and from a radiative transfer standpoint, serious errors in the evolution of the disks may develop. Therefore, even with all other things being equal, this difference alone could result in a different evolution of the spiral patterns, and thus of the outcome of gravitational instability. In what follows we will highlight the most important features of the two SPH codes and we will explicitly indicate in what ways the two codes differ and what is the expected outcome of such differences.

SPH is an approach to hydrodynamical modeling first developed by Lucy (1976) and Gingold & Monaghan (1977). It is a particle-based method that does not refer to grids for the calculation of hydrodynamical quantities: all forces and fluid properties are determined by moving particles, thereby eliminating numerically diffusive advective terms. The Boss & Myhill (1992) code is an Eulerian code, with all quantities defined on a spherical coordinate grid. The code is second-order accurate in both space and time, a crucial factor for keeping numerical diffusion at a tolerable level.

The basis of the SPH method is the Lagrangian representation and evolution of smoothly varying fluid quantities whose value is only known at disordered discrete points in space occupied by particles. Particles are the fundamental resolution elements comparable to cells in a grid. SPH operates through local summation operations over particles weighted with a smoothing kernel, W, that approximates a local integral. The smoothing operation provides a basis from which to obtain derivatives. Thus, estimates of density-related physical quantities and gradients are generated.

Both GASOLINE and Nelson's code use a fairly standard implementation of the hydrodynamical equations of motion for SPH (Monaghan 1992). The density at the location of each particle with index i is calculated from a sum over particle masses m_j

$$\rho_i = \sum_{j=1}^{n} m_j W_{ij}. \tag{2}$$

where j is an index running on the entire set of n particles. The momentum equation is expressed as

$$\frac{d\boldsymbol{v}_i}{dt} = -\sum_{j=1}^{n} m_j \left(\frac{P_i}{\rho_i^2} + \frac{P_j}{\rho_j^2} + \Pi_{ij} \right) \nabla_i W_{ij}, \tag{3}$$

where P_j is pressure, $\boldsymbol{v}_i$ is velocity and the artificial viscosity term is Π_{ij}.

The kernel is a standard B-spline with compact support in both codes (Hernquist & Katz 1987). The number of neighbors, or in other words, the number of particles around a given particle that are considered for smoothed sums, is fixed in GASOLINE at 32 and varies between 10 and 30 in the 2D version of Nelson's code, depending on the local flow.

2.2 Gravity solvers

Clearly gravity solvers represent a crucial aspect of simulations of self-gravitating disks. They need to be both accurate and efficient, and possibly parallelized in order to take advantage of modern computer architectures and permitting very high resolution calculations to be performed. Both GASOLINE and Nelson's code compute gravity using a tree-based solver, which is fast, easily parallelizable and a natural choice for a particle-based hydrodynamical such as SPH, since once a tree is built it can also be re-used as an efficient search method for hydrodynamical forces as well. Both codes use a modified versions of the binary tree described in Benz et al. (1990) which approximates the gravity of groups of distant particles in a multipole expansion while calculating interactions of nearby particles explicitly. Gravitational forces due to neighbor particles are softened to avoid divergences as particles pass near each other. The force calculation in tree algorithms requires work proportional to $\mathcal{O}(N\,log\,N)$, where N is the number of particles in the simulation, as opposed to work proportional to N^2 in "direct" N-Body algorithms where all gravitational forces between individual particles are computed directly. The drawback is that, except for very nearby particles whose interactions may be calculated as in direct summation codes, the forces are approximate rather than exact when using a tree. A particularly useful property of tree codes is the ability to efficiently calculate forces for a subset of the bodies. This is critical if there is a large range of time-scales in a simulation and multiple independent timesteps are employed (see below). At the cost of force calculations no longer being synchronized among the particles substantial gains in time-to-solution may be realized. Multiple timesteps are particularly important for applications where the primary interest and thus need for high spatial resolution tends to be focused on small regions within a larger simulated volume; a protoplanetary disk undergoing fragmentation locally is one such application. GASOLINE uses 4th (hexadecapole) rather than 2nd (quadrupole) order multipole moments (as used by most tree codes, including Nelson's) to represent the mass distribution in cells at each level of the tree. This results in less computation for the same level of accuracy: better pipelining, smaller interaction lists for each particle and reduced communication demands in parallel. The current implementation in GASOLINE

uses reduced moments that require only $n+1$ terms to be stored for the n^{th} moment. For a detailed discussion of the accuracy and efficiency of the tree algorithm as a function the order of the multipoles used, see Stadel (2001).

Relaxation effects compromise the attempt to model continuous fluids using particles. Both in GASOLINE and in Nelson's code the particle masses are effectively smoothed in space using the same spline kernels employed in the SPH calculation. This means that the gravitational forces vanish at zero separation and return to Newtonian $1/r^2$ at a separation of $\epsilon_i + \epsilon_j$ where ϵ_i is the gravitational softening applied to each particle. In this sense the gravitational forces are well matched to the SPH forces. However, in GASOLINE gravitational softening is constant over time and fixed at the beginning of the simulation, while in Nelson's code it is time-dependent and always equal to the local SPH smoothing length.

The use of adaptive softening in Nelson's code ensures that gravitational and pressure forces are always represented with the same resolution. Bate & Burkert (1997) have shown that when an imbalance between pressure and gravitational forces occurs, artificial fragmentation or suppression of physical fragmentation can arise. While Bate & Burkert (1997) found that such imbalance leads to spurious results when it occurs at a scale comparable with the local Jeans length of the system, more recently Nelson (2006) has shown that particle clumping was amplified for imbalances in softening/smoothing even when the Toomre wavelength was well resolved, which is a much more limiting codndition. When the gravitational softening is fixed over time, such as in GASOLINE, care has to be taken that this be comparable to the SPH smoothing length at the scale of the Jeans length. Mayer et al. (2005) choose the softening according to the latter prescription at the beginning of the simulation and set its value so that outside $10AU$ the softening drops to $\sim 1/2$ the local smoothing length. An argument can be made that later in the evolution, when strong overdensities develop along the spiral arms the SPH smoothing length drops significantly, becoming smaller than the gravitational softening, thereby degrading the propensity for numerical fragmentation. Both the initial softening/smoothing inequality and the later evolution of disks towards fragmentation were examined by Nelson (2006), with the result that to fragmentation was still enhanced, but after it began, simulations could be evolved much further, because the fragments did not continue to contract indefinitely but rather remained comparable in size to the fixed softening value. No specific tests of whether this occurs as well in the Mayer et al. work, or how the results may be affected, has yet been done. It may be of some note however, that the fragmentation in their work only occured in the outer half of their disks, where the force imbalances favor gravity, as seen in Nelson (2006).

An on going comparison between SPH and adaptive mesh refinement (AMR) codes conducted at different resolutions and particle softening is in preparation (Mayer et al., in preparation, see also Durisen et al. 2007) and may provide an independent check of the reliability of fragmentation in SPH. On the other hand, since this happens when the gas is optically thick, cooling

is also suppressed (see below), and this might be the dominant, physical effect in slowing down the collapse. Even so, compensating for insufficiencies in a physical model, using flaws in a numerical code, would seem to be, at best, undesirable. Adaptive softening is also not without flaws – particles have a time-dependent potential energy, which induces fluctuations in the potential that can in principle increase force errors, possibly affecting the accuracy of the integration. This is known to be problematic for purely gravitational simulations such as those of cosmic structure formation, but its consequences have not been studied systematically for the case of self-gravitating fluids. Recent work of Price & Monaghan (2006) has shown how adpative softening may be used while still conserving energy, but their technique has not yet seen wide adoption.

In the Boss & Myhill (1992) code, Poisson's equation is solved for the gravitational potential at each time step. This solution is achieved by using a spherical harmonic (Y_{lm}) expansion of the density and gravitational potential, with terms in the expansion up to $l, m = 32$ or 48 typically being used. Boss (2000, 2001) found that the number of terms in this expansion was just as important for robust clump formation as the spatial resolution. Because the computational effort involved scales as the number of terms squared, however, in practice this value cannot be increased much beyond 48 without having the Poisson solver dominate the effort. Boss (2005) showed that the introduction of point masses to represent very high density clumps led to better defined, more massive clumps, but the computational effort associated with introducing these point masses also led to an appreciable slowing the execution speeds.

2.3 Timestepping

Nelson's code uses the Runge-Kutta-Fahlberg method to evolve the equations of motion. It employs a global timestep for all particles in the disk, which was increased or decreased depending on the conditions in the simulations. The integrator is a first order accurate method with second order error control and the scheme provides limits on the second order error term in all of the various variables. Gasoline incorporates the timestep scheme described as Kick-Drift-Kick (KDK) (see Wadsley et al. 2004). Without gas forces this is a symplectic leap-frog integration, which ensures the conservation of total energy, this being not guaranteed with the Runge-Kutta method (Quinn et al. 1997; Tremaine et al. 2003), though much better conservation can be had when a single time step for all particles is used, as was done in Nelson (2000). The leap-frog scheme requires only one force evaluation and minimum storage. GASOLINE uses multiple timesteps, hence at any given time different particles in the disk can be evolved with different timesteps. The base (maximum) timestep is divided in a hierarchy of smaller steps (rungs), with different particles being assigned to different rungs. This allows to reach a much smaller step size when it is required, allowing to probe a much higher dynamic range and follow correctly the dynamics of regions with very high densities. The drawback is that the

scheme is no longer strictly symplectic if particles change rungs during the integration which they generally must do to satisfy their individual timestep criteria. Adaptivity in the time integration, hence the ability to achieve small timesteps than the dynamics or hydrodynamics require so, can be important to model correctly the formation and evolution of overdensities and clumps. In fact, if the step size is not small enough the acceleration inside the overdensities, that goes as $1/\Delta t^2$, can be underestimated. This is equivalent to underestimate the self-gravity of clumps and can in principle lead to their artificial dissolution, although no systematic tests have ever been performed. GASOLINE uses a standard timestep criterion based on the particle acceleration (see Wadsley et al. 2004) and for gas particles, the Courant condition and the expansion cooling rate. Nelson's code adopts the Courant condition as well for hydrodynamical forces and addituonally a set of constraints based on the position and velocities of particles. If the latter are not met after a timestep, the scheme went back and tries again with a smaller timestep.

The Boss & Myhill (1992) code uses a single-size timestep based on the Courant condition, and uses a predictor-corrector method to achieve second-order accuracy in time.

2.4 Artificial viscosity

Most hydrodynamic methods need artificial viscosity to stabilize the flow by avoiding particle interpenetration and to resolve in an approximate manner the physical dissipation present in shocks, and SPH is no exception. Both Mayer et al. (2005) and Nelson (2000) use bulk and von Neumann-Richtmyer (so called '$\bar{\alpha}$' and 'β') viscosities to simulate viscous pressures which are linear and quadratic in the velocity divergence. They both incorporate a switch (see Balsara 1995) that acts to reduce substantially the large undesirable shear component associated with the standard form.

In both GASOLINE and Nelson's code the artificial viscosity term reads

$$\Pi_{ij} = \begin{cases} \frac{-\alpha\frac{1}{2}(c_i+c_j)\mu_{ij}+\beta\mu_{ij}^2}{\frac{1}{2}(\rho_i+\rho j)} & \text{for } \boldsymbol{v}_{ij}\cdot\boldsymbol{r}_{ij} < 0, \\ 0 & \text{otherwise,} \end{cases} \tag{4}$$

$$\text{where } \mu_{ij} = \frac{h(\boldsymbol{v}_{ij}\cdot\boldsymbol{r}_{ij})}{\boldsymbol{r}_{ij}^2 + 0.01(h_i+h_j)^2}, \tag{5}$$

where $\boldsymbol{r}_{ij} = \boldsymbol{r}_i - \boldsymbol{r}_j$, $\boldsymbol{v}_{ij} = \boldsymbol{v}_i - \boldsymbol{v}_j$, and c_j is the sound speed. $\alpha = 1$ and $\beta = 2$ are standard values of the coefficients of artificial viscosity, known to result in acceptable dissipative behavior across a wide variety of test problems.

In protoplanetary disks, Mach numbers are high (of order 10-20) although shocks are not as strong (i.e. the density jumps are not as pronounced) as when gas collapses or collides with other gas along nearly radial trajectories such as in cosmological structure formation. This is important because it

means that the standard settings for the viscous coefficients may be higher than strictly necessary for correct evolution of the flow. Since artificial viscosity is essentially a nuisance with regard to improving the modeling of the hydrodynamical flow, any improvements which decrease the importance of unphysical side effects, while retaining the required stability and dissipative effects of the code, are desirable.

Mayer et al. (2004) have therefore experimented with lowering the coefficients of artificial viscosity, finding that for e.g. $\alpha = 0.5$ and $\beta = 0$ or $\alpha = 0.5$ and $\beta = 1$ fragmentation is more vigorous. However, the simulations of binary protoplanetary disks in Mayer et al. (2005) were designed following a conservative approach, hence the standard values $\alpha = 1$ and $\beta = 2$ were employed. They do, however, include a modification due to Balsara (1995), to modify the computation of the velocity divergence from its usual form by multiplying the above equation by a correction factor

$$f_i = \frac{|(\nabla \cdot \mathbf{v_i})|}{|(\nabla \cdot \mathbf{v_i})| + |(\nabla \times \mathbf{v_i})| + 0.0001 c_i/h_i}. \quad (6)$$

to reduce shear viscosity. This factor is near unity when the flow is strongly compressive, but near zero in shear flows. In the simulations of Nelson et al. (2000) and Nelson (2000), the typical reduction of viscosity due to this term is a factor of three or better.

Nelson's code starts from the same formulation of artificial viscosity shown above (except that surface density replaces volume density), modified by the same Balsara shear factor, but then also includes a second treatment to obtain a locally varying artificial viscosity. This treatment is due to Morris and Monaghan (1997), who implemented a time dependence to the coefficient $\bar{\alpha}$ that allows growth in regions where it is physically appropriate (strong compressions) and decay in quiescent regions where it is inappropriate. The decay takes place over distances of a few SPH smoothing lengths, after which the coefficient stabilizes to a constant, quiescent value. Nelson adopts a formulation including both the $\bar{\alpha}$ and β terms, where $\bar{\alpha}/\beta \equiv 0.5$, but the magnitudes of the coefficients vary in time and space according to the Morris & Monaghan formulation. Thus, except in strongly compressing regions (shocks) where it is required to stabilize the flow, artificial viscous dissipation is minimized.

In GASOLINE, only the Balsara correction term is added. Therefore, in general the GASOLINE simulations presented in Mayer et al. (2005) should be more diffusive, which should go in the direction of suppressing fragmentation if all other aspects of the modeling are the same. Figure 2 supports the claim of Mayer et al. (2004) on the effect of artificial viscosity by showing that even the simple omission of the Balsara term to reduce spurious shear viscosity can suppress fragmentation in an otherwise fragmenting disk. However, we note that the effect of artificial viscosity is more subtle than this, and that tests such as those of Figure 2 probably address only the impact of viscosity on the transition between mild overdensities and those strong enough to begin collapsing. Once they start collapsing the prevailing effect of artificial viscosity

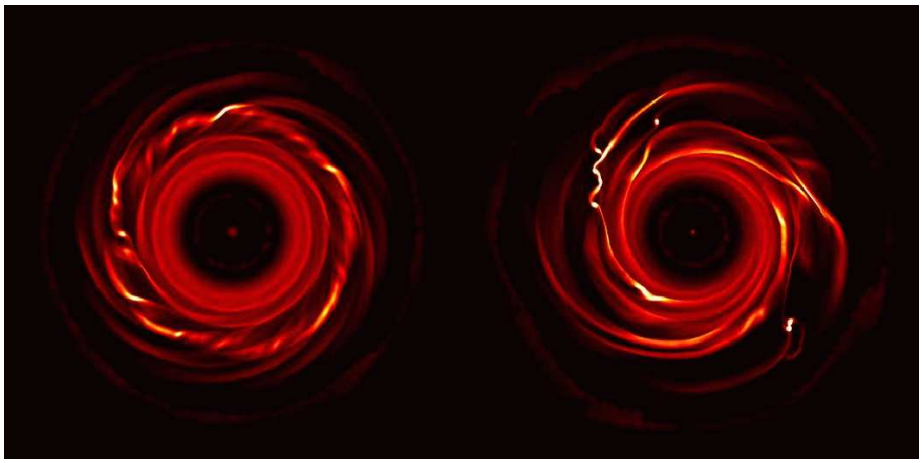

Fig. 2. Color coded density maps of two isothermal runs evolved with 1 million SPH particles. The disk starts with a minimum Toomre parameter approaching $Q \sim 1$. The snapshots after about 8 orbital times at 10 AU, i.e. about 240 years, are shown. On the left a run without the Balsara correction term is shown, on the right the same disk is evolved with the Balsara term on.

could actually be to enhance the growth and survival of the clumps by taking kinetic energy out of the system.

Artificial viscosity, be it explicitly inserted or implicit to the code, is one way in which actual physical processes ocurring on the sub-grid scale, such as shock front heating and dissipation, can be included in the calculation. A tensor formulation artificial viscosity is included in the Boss & Myhill (1992) code, but is generally not used in the disk instability models, except to discern the extent to which artificial viscosity can suppress fragmentation (Boss 2006b). Numerical stability is maintained instead by using as small a fraction of the Courant time step as is needed, sometimes as low as 1% of the Courant value. Boss (2006b) showed that his code reproduced an analytical (Burgers) shock wave solution nearly as well without any artificial viscosity as when a standard amount ($C_Q = 1$, see Boss & Myhill 1992) of artificial viscosity was employed, implying that the intrinsic numerical viscosity of his code was sufficient to stabilize such a shock front. Tests on the full set of hydrodynamic equations have not been published.

2.5 Internal energy equation

Both GASOLINE and Nelson's code employ the following energy equation (called "asymmetric"), advocated by Evrard (1990) and Benz (1990), which conserves energy exactly in each pairwise exchange and is dependent only on the local particle pressure,

$$\frac{d\ u_i}{dt} = \frac{P_i}{\rho_i^2} \sum_{j=1}^{n} m_j \boldsymbol{v}_{ij} \cdot \nabla_i W_{ij}, \tag{7}$$

where u_i is the internal energy of particle i, which is equal to $1/(\gamma - 1)P_i/\rho_i$ for an ideal gas. In this formulation entropy is closely conserved making it similar to alternative entropy integration approaches, such as that proposed by Springel & Hernquist (2002). The equation above includes only the part related to PdV work, while the full energy equation has a term due to artificial viscosity and one due to cooling to be discussed below.

The adiabatic index γ is different in Nelson (2000) and Mayer et al. (2005) because Nelson (2000) perform only two dimensional simulations, In both cases the value of γ appropriate for a gas at temperatures $T < 1000$ K in which rotational transitions are active, but not the vibrational ones, is assumed. Because of the differences in dimensionality, this assumption yields $\gamma = 1.4$ in 3D for the pure hydrogen gas (i.e. average molecular weight of 2.0) assumed by Mayer et al. and $\gamma \sim 1.53$ in 2D, for the solar composition gas (average molecular weight 2.31) used by Nelson (see also Nelson 2006 for a discussion of issues that affect the ratio of specific heats in 2D calculations). A value of $\gamma = 1.42$ was incorporated into the vertical structure models used in Nelson (2000) in order to remain consistent, since the assumptions implicit in that calculation required a 3D treatment. Other published work adopts $\gamma = 5/3$ (Rice et al. 2003a, 2005; Cai et al. 2006a,b). As we explain below, the value of γ can have an impact on whether fragmentation occurs or not in a self-gravitating disk, both isolated and in a binary system. A recent paper (Boley et al. 2006) explains how using just one or two values of the adiabatic independently on the actual temperature and density of the gas is probably a poor approximation of the real physics of molecular hydrogen transitions which can affect the outcome of gravitational instability. Future work will need to asess that.

A term dependent on artificial viscosity is added to eq. (7)

$$\sum_{j=1}^{n} m_j \frac{1}{2} \Pi_{ij} \boldsymbol{v}_{ij} \cdot \nabla_i W_{ij} \tag{8}$$

(see eq. (4) and (5) for the definition of Π_{ij}).
This term allows the modeling of irreversible heating occurring in shocks and the related changes in the entropy of the fluid.

If no radiative cooling is included the resulting model is sometimes dubbed "adiabatic" to distinguish it from the "isentropic" cases in which no irreversible heating is included (Durisen et al. 2007). However, in the simulations of binary protoplanetary disks of Mayer et al. (2005) and Nelson (2000) a cooling term is always present. The cooling term is described in the following section.

Boss & Myhill (1992) code an equation for the specific internal energy with explicit time differencing, in the same manner as the other hydrody-

namic equations are solved. This energy equation includes the effects of compressional heating and cooling and of radiative transfer, in either the diffusion or Eddington approximations. In the latter case, a separate equation for the mean intensity must be solved. In the diffusion approximation, the energy equation is solved by Boss's code (Boss 2001) in the form

$$\frac{\partial(\rho E)}{\partial t} + \nabla \cdot (\rho E \mathbf{v}) = -p \nabla \cdot \mathbf{v} + \nabla \cdot \left[\frac{4}{3\kappa\rho} \nabla (\sigma T^4) \right]$$

where ρ = gas density, $\mathbf{v}$ = fluid velocity, E = specific internal energy = $E(\rho, T)$, p = gas pressure = $p(\rho, T)$, κ = Rosseland mean opacity of gas and dust = $\kappa(\rho, T)$, T = gas and dust temperature, and σ = Stefan-Boltzmann constant = 5.67×10^{-5} cgs. The diffusion approximation energy equation has been used for all of Boss's disk instability models with radiative transfer to date. However, the Eddington approximation energy equation was used to derive the initial quasi-steady state thermal profiles (Boss 1996) used for the initial conditions in Boss's disk instability models. In the Eddington approximation code, the energy equation is

$$\frac{\partial(\rho E)}{\partial t} + \nabla \cdot (\rho E \mathbf{v}) = -p \nabla \cdot \mathbf{v} + L$$

where L is the rate of change internal energy due to radiative transfer. The formulation of L depends on the optical depth τ as

$$L = 4\pi\kappa\rho(J - B) \quad ..... \quad \tau < \tau_c$$

$$L = \frac{4\pi}{3} \nabla \cdot (\frac{1}{\kappa\rho} \nabla J) \quad ..... \quad \tau > \tau_c$$

where τ_c is a critical value for the optical depth ($\tau_c \sim 1$), κ is the mean opacity, J is the mean intensity, and $B = \sigma T^4/\pi$ is the Planck function. The mean intensity J is determined by the equation

$$\frac{1}{3} \frac{1}{\kappa\rho} \nabla \cdot (\frac{1}{\kappa\rho} \nabla J) - J = -B$$

The computational burden associated with the iterative solution of the mean intensity equation in the Eddington approximation has so far precluded its use in disk instability models with the high spatial resolution needed to follow the evolution over many orbital periods. Because of the high optical depths at the midplane (up to $\tau \sim 10^4$) of these disks, however, the diffusion approximation is valid near the critical disk midplane, and radiative transfer in the diffusion approximation imposes little added computational burden.

2.6 Cooling in the simulations

Nelson et al. (2000) and Nelson (2000) requires that the disk be in instantaneous vertical entropy equilibrium and instantaneous vertical thermal balance in order to determine its structure. This implicitly assumes that the disk will be convectively unstable vertically over a short timescale and quickly restore thermal balance. Convection is expected given the high optical depths of massive gravitationally unstable disks (Ruden & Pollack 1996); vigorous vertical currents with features resemblant of convective instabilities have been indeed observed in massive protoplanetary disks modeled with either SPH and grid codes (Boss 2003, 2004; Mayer et al. 2006). Under these assumptions the gas is locally (and instantaneously) adiabatic as a function of z. In an adiabatic medium, the gas pressure and density are related by $p = K\rho^{\gamma}$ and the heat capacity of the gas, C_V, is a constant (by extension, also the ratio of specific heats, γ, see above). In fact, this will not be the case in general because, in various temperature regimes, molecular hydrogen will have active rotational or vibrational modes, it may dissociate into atomic form or it may become ionized.

From the now known (ρ, T) structure, Nelson et al. derive the temperature of the disk photosphere by a numerical integration of the optical depth, τ, from $z = \infty$ to the altitude at which the optical depth becomes $\tau = 2/3$

$$\tau = 2/3 = \int_{\infty}^{z_{phot}} \rho(z)\kappa(\rho, T)dz. \tag{9}$$

In optically thin regions, for which $\tau < 2/3$ at the midplane, they assume the photosphere temperature is that of the midplane. The photosphere temperature is then tabulated as a function of the three input variables radius, surface density and specific internal energy. At each time the photosphere temperature is determined for each particle from such table and used to cool the particle as a blackbody at that temperature. The cooling of any particular particle proceeds as

$$\frac{du_i}{dt} = \frac{-2\sigma_R T_{eff}^4}{\Sigma_j} \tag{10}$$

where σ_R is the Stefan-Boltzmann constant, u_i and Σ_i are the specific internal energy and surface density of particle i and T_{eff} is its photospheric temperature. The factor of two accounts for the two surfaces of the disk. On every particle, the condition that the temperature (both midplane and photosphere) never falls below the 3 K cosmic background temperature is enfoced. Rosseland mean opacities from tables of Pollack, McKay & Christofferson (1985) are used. Opacities for packets of matter above the grain destruction temperature are taken from Alexander & Ferguson (1994).

In parts of the disk where the calculated midplane temperature is greater than dust vaporization temperature, the opacity is temporarily reduced to $\sim 5\%$ of its tabulated values over the entire column above and below that

point in the disk. This accounts for the fact that dust formation, after once being vaporized, may occur at rates slower than the timescales for vertical transport through the column. In other regions of the disk we assume that the opacity remains unaffected.

Cooling is treated very differently in Mayer et al. (2005). Cooling is independent on distance from the midplane also in this case (so there is no dependence on z, as if there was constant thermal equilibrium vertically) but there is an explicit dependence on the distance from the center. The cooling term is proportional to the local orbital time, $t_{orb} = 2\pi/\Omega$, where Ω is the angular velocity, via the following equation

$$\Lambda = dU/dt = U/A\Omega^{-1} \tag{11}$$

The disk orbital time is a natural characteristic timescale for spiral modes developing in a rotating disk. Cooling is switched off inside 5 AU in order to maintain temperatures high enough to be comparable to those in protosolar nebula models (e.g. Boss 1998), and in regions reaching a density above 10^{-10} g/cm^3 to account for the local high optical depth; indeed according to the simulations of Boss (2002) with flux-limited diffusion the temperature of the gas evolves nearly adiabatically above such densities. In practice in these regions the gas simply obeys eq. (7) with the artificial viscosity term (8). Mayer et al. (2005) considered cooling times going from 0.3 to 1.5 the local orbital time. The jury is still out on whether the cooling times adopted here are credible or excessively short. Recent calculations by Boss (2002, 2004), Johnson & Gammie (2003) and Mayer et al. (2006), which use different approximate treatments of radiative transfer, do find cooling times of this magnitude through a combination of radiative losses and convection, but other works such as those of Mejia et al. (2005), Cai et al. (2006) and Boley et al. (2006) encounter longer cooling times and never find fragmentation. The cooling times used in Nelson (2000) are about 25 times longer than the typical orbital time in the region $(5 - 10$ AU), hence they were much longer than in Mayer et al. (2005). As we shall see, this will have profound implications on the final outcome of the simulations.

In work in progress, one of the authors, L.Mayer, has begun performing simulations of binary protoplanetary disks using the new flux-limited diffusion scheme for radiative transfer adopted in Mayer et al. (2006), which adopts the flux-limiter of Bodenheimer et al. (1991) in the transition between optically thick and optically thin regions of the disk. The disk then radiates as a blackbody at the edge, with the radiative efficiency being modulated by a parameter that defines how large is the emitting surface area, or in other words, the part of the disk that qualifies as edge. In section 5 we briefly describe some preliminary results of these new calculations.

Boss (2001) noted that in his diffusion approximation models, the radiative flux term is set equal to zero in regions where the optical depth τ drops below 10, so that the diffusion approximation does not affect the solution in low

optical depth regions where it is not valid. This assumption is intended to err on the conservative side of limiting radiative cooling. A test model (Boss 2001) that varied this assumption by using a critical $\tau_c = 1$ instead of 10 led to essentially the same results as with $\tau_c = 10$, implying insensitivity of the results to this assumption. Another test model (Boss 2001) used a more detailed flux-limiter to ensure that the radiative energy flux did not exceed the speed of light (specifically, that the magnitude of the net flux vector $\boldsymbol{H}$ did not exceed the mean intensity J), and also yielded essentially the same results as the model with the standard assumptions. In low optical depth regions such as the disk envelope, the gas and dust temperature is assumed to be 50 K.

In the Boss (2006b) models, the disk was assumed to be embedded in an infalling envelope of gas and dust that formed a thermal bath with a temperature of 50K. Thus the effective surface boundary condition on the disk is 50K. Boss (2004a) found that convective-like motions occurred in the models with a vigor sufficient to transport the heat produced at the midplane by clump formation to the surface of the disk, where it is effectively assumed to be radiated away into the protostellar envelope. This code also employs a full thermodynamical description of the gas, including detailed equations of state for the gas pressure, the specific internal energy, and the dust grain and atomic opacities in the Rosseland mean approximation.

Molecular hydrogen dissociation is treated, as well as a parameterized treatment of the transition between para- and ortho-hydrogen. Linear interpolation from 100 K to 200K is used to represent the variations between a specific internal energy per gram of hydrogen of $3/2R_gT/\mu$ (where R_g is the gas constant, T is the temperature, and $\mu = 2$ is the mean molecular weight for molecular hydrogen) for temperatures less than 100 K and of $5/2R_gT/\mu$ for temperatures above 200 K. No discontinuities are present in this internal energy equation of state, which has been used in all of Boss's disk instability models.

Rafikov (2006) has noted that while vigorous convection is possible in disks, the disk photosphere will limit the disk's radiative losses and so may control the outcome of a disk instability. Numerical experiments designed to further test the radiative transfer treatment employed in the Boss models (beyond the tests described above) have been completed, and other models are underway (Boss 2007, in preparation). Understanding the extent to which the surface of a fully 3D disk, with optical depths that vary in all directions and with corrugations that may shield the disk's surface from the central protostar and other regions of the disk, requires a fully numerical treatment and is not amenable to a simple analytical approach.

3 Initial and Boundary Conditions

Here we describe the initial and boundary conditions for the models, focusing on the different choices made by different workers. These choices include (1) density and temperature profiles of the disks, (2) disk masses and Toomre parameters, (3) spatial resolution, (4) the boundary conditions, and (5) the orbital configuration in the binary experiments.

One important difference to point out is that Mayer et al. (2005) start their binary simulations after growing the individual disks in isolation. The disk mass is grown until it reaches the desired value while keeping the temperature of the particles constant over time. The Toomre parameter is prevented from falling below 2 by setting the temperature of the disk sufficiently high at the start. This way the initial conditions used for the binary experiments are those of a gravitationally stable disk. The Toomre parameter is then lowered to a value in the range $1.4 - 2$ by resetting the temperature of the particles before placing the disk on the binary orbit (the temperature is set to 65 K, hence the Toomre parameter will depend on the mass of the disk, see below in the next two sections). As the disk evolves in isolation, it expands slightly, losing the sharp outer edges. The inner hole also fills up partially, but most of the particles remain on very similar orbits. Once the disk is placed on an orbit around a companion disk, the system is further evolved using the full energy equation plus a cooling term dependent on the orbital time, therefore including adiabatic compression and expansion, irreversible shock heating and radiative cooling. Nelson (2000) do not grow the disk but start with a treatment that also solves the full energy equation but treats the cooling term differently (see above).

In both Mayer et al. (2005) and Nelson (2000) matter is set up on initially circular orbits assuming rotational equilibrium in the disk. The central star is modeled by a single massive, softened particle. Radial velocities are set to zero. Gravitational and pressure forces are balanced by centrifugal forces including the small contribution of the disk mass.The magnitudes of the pressure and self-gravitational forces are small compared to the stellar term, therefore the disk is nearly Keplerian in character. No explicit initial perturbations are assumed beyond computational roundoff error in either Mayer et al. (2005) or Nelson (2000). Due to the discrete representation of the fluid variables, this perturbation translates to a noise level of order $\sim 10^{-3} - 10^{-2}$ for the SPH calculations. The relatively large amplitude of the noise originates from the fact that the hydrodynamic quantities are smoothed using a comparatively small number of neighbors (see Herant & Woosley 1994). An increase in the number of particles does not necessarily decrease the noise unless the smoothing extends over a larger number of neighbors. This perturbation provides the initial seed that can be amplified by gravitational instability. The initial disk model in Boss (2006b) is rotating with a near-Keplerian angular velocity chosen to maximize the stability of the initial equilibrium state, with zero translational motions. The envelope above the disk, however, is assumed to

be falling down with free-fall velocities but with the same angular velocity profile as the rotating disk. Random cell-to-cell noise at the level of 10% is introduced to the disk density to seed the cloud with non-axisymmetry at a controlled level.

3.1 Density and temperature profiles

Mayer et al. (2005) grow the disks slowly over time until the desired mass is reached. The initial disk models extend from 4 to 20 AU and have a surface density profile $\Sigma(r) \sim r^{-1.5}$ with an exponential cut-off at both the inner and outer edge. The initial vertical density structure of the disks is imposed by assuming hydrostatic equilibrium for an assumed temperature profile $T(r)$. Nelson (2000) adopts a power law for the initial disk surface density profile of the form

$$\Sigma(r) = \Sigma_0 \left[1 + \left(\frac{r}{r_c}\right)^2\right]^{-\frac{p}{2}}, \tag{12}$$

where p is 3/2 and Σ_0 is the central surface density of the disk, which is determined once the total disk mass is assigned. The Nelson (2000) disk extends from 0.3 to 15 AU, and the core radius used for the power laws to the value $r_c = 1$ AU. The stars had Plummer softening of 0.2 AU each, while a softening length of 2 AU was used with the spline kernel softening in Mayer et al. (2005).

The shape of the initial temperature profile in Mayer et al. (2005) is similar to that used by Boss (1998, 2001) and is shown in Figure 3 together with the profiles of several runs with either binary or isolated disks after a few orbits of evolution.

The temperature depends only on radius, so there is no difference between midplane and an atmosphere. Between 5 and 10 AU the temperature varies as $\sim r^{-1/2}$, which resembles the slope obtained if viscous accretion onto the central star is the key driver of disk evolution (Boss 1993). Between 4 and 5 AU the temperature profile rises more steeply, in agreement with the 2D radiative transfer calculations of Boss (1996), while it smoothly flattens out for $R > 10$ AU and reaches a constant minimum temperature (an exponential cut-off is used). The initial temperature profile of Nelson (2000) is instead

$$T(r) = T_0 \left[1 + \left(\frac{r}{r_c}\right)^2\right]^{-\frac{q}{2}}, \tag{13}$$

where q is 1/2 and T_0 is the central temperature, which is determined once the minimum desired Toomre parameter, and hence the minimum temperature, is determined (see above).

In Mayer et al. (2005) the minimum temperature is fixed to 65 K. It is implicitly assumed that the disk temperature is related to the temperature of

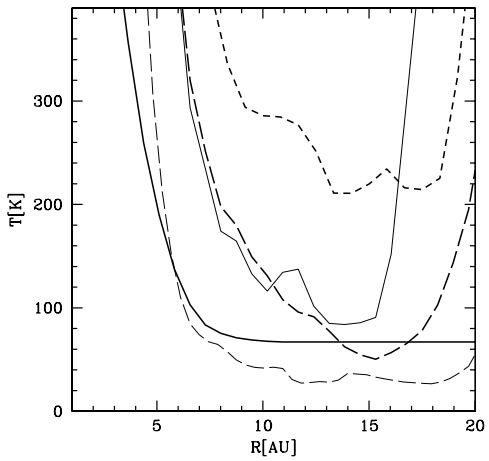

Fig. 3. Azimuthally averaged mid-plane temperature profiles at the time of maximum amplitude of the overdensities (at between 120 years and 2000 years of evolution depending on the model) in some of the runs described in Mayer et al. (2005). The initial temperature profile is shown by the thick solid line. We show the results for a run with two massive disks ($M = 0.1 M_{\odot}$, thick short-dashed line, the disks do not fragment) at a separation of about 60 AU, a run with just one of these two disks in isolation (thin long-dashed line, disk fragments), a run with the same massive disks at a larger separation of 116 AU (disks fragment) and a run with two light disks ($M = 0.01 M_{\odot}$, the disks do not fragment) at a separation of 60 AU. The runs adopt cooling times in the range $0.5 - 1.5$ the local orbital time. A smaller separation and a larger disk mass both favour stronger spiral shocks and hence a larger temperature increase during the evolution.

the embedding molecular cloud core from which the disk would be accreting material (Boss 1996). Note that, at least for the protosolar nebula, 50 K is probably a conservative upper limit for the characteristic temperature at $R > 10$ AU based on the chemical composition of comets in the Solar System (temperatures as low as 20 K are suggested in the recent study by Kawakita et al. 2001). Outer temperatures between 30 and 70 K are found also for several T Tauri disks by modeling their spectral energy distribution assuming a mixture of gas and dust and including radiative transfer (D'Alessio et al. 2001).

In the Boss (2006b) models, the initial disk is an approximate semi-analytic equilibrium model (Boss 1993) with a temperature profile derived from the Eddingtion approximation radiative transfer models of Boss (1996). The outer disk temperatures were taken to be either 40K, 50K, 60K, 70K, or 80K, in order to test the effects of starting with disks that were either marginally gravitationally unstable (40K, 50K) or gravitationally stable (60K, 70K, 80K). The

disk temperature is not allowed to fall below its initial value, an approximation that errs on the side of suppressing fragmentation.

Figure 4 shows the initial radial temperature profile for the models with an outer disk temperature of 80 K, as was assumed in the Boss (2006b) model shown in Figure 7. The temperature rises strongly toward the protostar at 0 AU because of the heating associated with mass accretion onto the disk from the protostellar envelope and onto the central protostar from the disk (Boss 1993, 1996). The temperature distributions in Boss (1993, 1996) are steady state solutions for axisymmetric (2D) protoplanetary disks with varied disk and stellar masses, opacities, and other parameters.

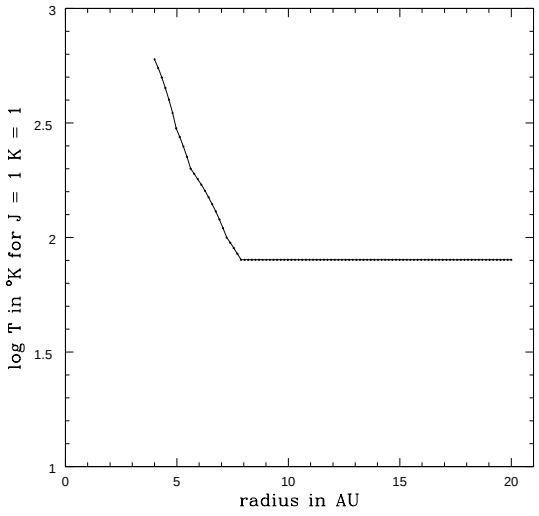

Fig. 4. Initial radial temperature profile for the midplane of the Boss (2006b) models with outer disk temperatures of 80K. Each dot corresponds to a radial grid point (100 in all) distributed between 4 AU and 20 AU. This initial profile was used for the model shown in Figure 7.

3.2 Disk masses and Toomre parameters

Both Nelson (2000) and Mayer et al. (2005) consider a system composed of two disks with their central stars, while Boss (2006) models one system with a disk and star, and the companion with just a star. The two disks have equal masses, $0.05 M_{\odot}$, in Nelson (2000), while Mayer et al. (2005) consider a range of disk masses encompassing models from as light as the lowest expected values of the minimum mass solar nebula ($0.012 M_{\odot}$) to as massive as the heaviest among T Tauri disks ($0.1 M_{\odot}$. A few simulations with disks having unequal masses were performed by Mayer et al. (2005), while in the majority of the runs the disks have the same mass. Boss (2006) considers systems having equal mass stars. The mass of the central star is $0.1 M_{\odot}$ in Mayer et al. (2005) and $0.5 M_{\odot}$ in Nelson (2000). The minimum Toomre parameter is ~ 1.5 in Nelson (2000) achieved just inside the outer edge of the disk, at $10 - 12$ AU, while it is $Q_{min} \sim 1.4$ or higher in Mayer et al. (2005) at the disk edge, where the temperature also falls to its minimum. The details of the individual models can be found in Mayer et al. (2005). The initial surface densities and Toomre profiles differ between the two works and give rise to a different susceptibility to various channels by which non-axisymmetric models can grow. In Nelson (2000), Q is nearly flat over the largest portion of the disk, with a steep rise at small radii and a shallow increase towards the outer edge of the disk. In Mayer et al. (2005), disks are constructed in such a way that they begin with a steep inner rise of Q, which decreases outwards and reaches its minimum at the disk edge (Mayer et al. 2004). However, as the disk grows in mass the Q profile changes; its minimum shifts inwards, near 15 AU, so that the overall profile becomes quite similar to that of Nelson (2000) by the beginning of the simulations. We refer to Mayer et al. (2004) and Nelson et al. (2000) for details on the Q profiles.

In the Boss (2006b) models, the disk mass is $0.091 M_{\odot}$ and the central protostar has a mass of $1 M_{\odot}$. Because the outer disk temperatures in different models are varied from 40K to 80K, the minimum value of the Toomre Q parameter varies from 1.3 to 1.9 in the models.

Figure 5 shows the radial profile of the Toomre Q parameter for the Boss (2006b) models with an outer disk temperature of 80K, the same as for the model shown in Figures 4 and Figure 7. The disk is very stable to gravitational perturbations in its inner regions, because of the high inner disk temperatures (Figure 4), but drops to a minimum value of 1.9 in the outer disk.

3.3 Numerical resolution

Nelson (2000) employs 60000 particles per disk in his 2D simulations, while Mayer et al. (2005) used 200000 particles per disk. Due to the differences in dimensionality, the mass resolution along the disk midplane is quite similar, so in this respect the two simulations are quite comparable. The gravitational softening is fixed at $\sim 0.06 AU$ in Mayer et al. (2005), while it can become

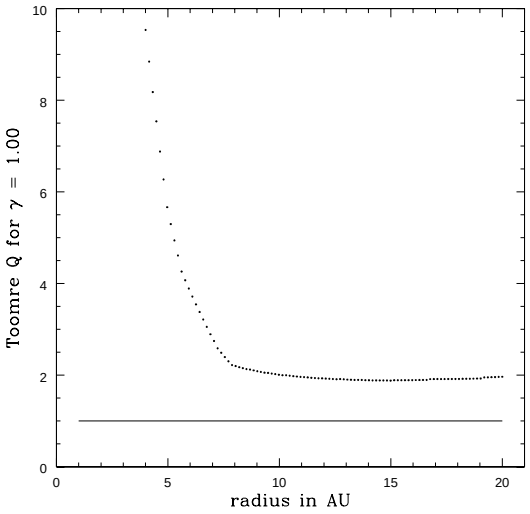

Fig. 5. Initial Toomre Q profile for the midplane of the Boss (2006b) models with outer disk temperatures of 80K, used for the model shown in Figure 7

smaller than that in Nelson (2000) in overdense regions forming during the simulation.

Boss (2006b) used a grid with either $100 \times 22 \times 256 = 0.56 \times 10^6$ or with $100 \times 22 \times 512 = 1.1 \times 10^6$ grid points, distributed over the top hemisphere of the calculational grid, and either 32 or 48 terms in the spherical harmonic expansion for the gravitational potential.

3.4 Boundary conditions

Mayer et al. (2005) adopt no boundary conditions at all in their disks. The central star is free to move in response to deviations of the gravitational potential of the disk from the initial equilibrium and gas particles can get as close as resolution allows. Although such a choice is not ideal from the point of view of computational efficiency, since particles nearest to the center have the shortest timesteps, this should reduce fluctuations in the inner density and pressure profiles due to the sudden removal of particles. Nelson (2000) instead implements an inner boundary condition by treating the central star as a sink

particle, namely a particle that absorbs the mass and momentum of particles falling below some threshold radius. He uses an accretion radius of 0.2 AU as a compromise between the numerical requirement that the integration time step not be so small that long period evolution cannot be followed and the desire to model as large a radial extent of the disk as possible. The gravitational softening of the central star in Mayer et al. (2005) is 2 AU, which for a spline kernel softening means that effectively the force resolution is 4 AU. In both Mayer et al. (2005) and Nelson (2000) the initial location of the innermost ring of particles lies slightly outside the inner accretion radius or gravitational softening of the star. There is no outer boundary condition in either of these works.

In the Boss (2006b) models, the inner boundary at 4 AU is allowed to remove mass and angular momentum from the grid and deposit it onto the central protostar. The outer boundary at 20 AU is fixed in space, and attempts to capture gas which reaches it while suppressing its tendency to bounce back inward. As a result of the strong tidal forces by the binary companions in Boss (2006b), disk gas which attempts to flow outward becomes artificially trapped in the outermost shell of cells. Thus any clumps observed on the or close to the outer boundary of the Boss (2006b) are artifacts of the outer boundary conditions and should disregarded.

3.5 Orbital parameters

Both Mayer et al. (2005) and Nelson (2000) consider coplanar disks corotating with their orbital motion as expected from fragmentation of a cloud core (Bate 2000). If core formation and fragmentation is a highly dynamical process as recent simulations of gravoturbulent molecular cloud collapse suggest, so that several cores interact strongly during collapse, more complicated orbital configurations will arise. These will need to be explored in the future. Fast close encounters between disks will also occur in the latter scenario, as Lodato et al. (2007) have investigated. In Nelson (2000) the semi-major axis is set to an initial value of 50 AU and the orbit has an eccentricity of 0.3. Mayer et al. (2005) consider a more circular orbit ($e = 0.14$) and two different semi-major axes, of 58 and 116 AU. The calculation starts with the companion disk being at the apoastron of the orbit.

Boss (2006b) considers only a single disk in his models, with the binary companion being a point mass protostar. The binary companion orbits were chosen to have semimajor axes of either 50 or 100 AU, namely comparable to those chosen by Mayer et al. (2005), to have eccentricities of either 0.25 or 0.5, and to having the calculation start off with the binary companion at either apoastron or at periastron in its orbit. The models assume that the mass of the binary companion is the same as that of the central protostar, $1 M_{\odot}$.

Note that in the Boss (2006b) models, the binary semimajor axis is defined to be equal to the radial separation between the two protostars, so that in a model with a semimajor axis of 50 AU and an eccentricity of 0.5, the closest

approach between the two protostars is 25 AU, just beyond the edge of the 20 AU-radius disk that is being perturbed by the binary companion. If the binary companion had a similar size disk, these disks would collide, but the binary companion is assumed to be a diskless point mass in all of the Boss (2006b) models.

4 Gravitational instability in binary systems

4.1 Does binarity help or suppress disk fragmentation?

The three studies seemingly reached very different conclusions regarding the role of binary companions in disk instabilities. Nelson (2000) found no aid to fragmentation, Mayer et al. (2005) found fragmentation in a few cases but also found an indication that binarity might reduce the susceptibility to fragment, while Boss (2006b) found fragmentation to be enhanced by binarity. However, we shall analyze in more detail these differences, trying to understand their causes.

As we have seen in the previous sections, there are many differences in the codes and setup of the numerical experiments. Mayer et al. (2005) performed a larger number of experiments, thus exploring a larger parameter space in terms of initial conditions. Nelson (2000) and Boss (2006b) had more realistic treatments of radiation transfer, while Boss (2006b) ran the highest resolution experiments. Disk thermodynamics is crucial for the outcome of gravitational instability. Fragmentation will occur only if cooling times are comparable to the orbital time. Therefore, leaving alone all the other differences, the simple fact that Nelson (2000) had cooling times in a large fraction of his disks that were a factor of 10 times longer than the orbital times can explain why fragmentation did not occur in his models. With such long cooling times, disks will not fragment in isolation, no matter how strong is the spiral structure appearing in the disk, and thus irrespective of whether this structure is spontaneous or is tidally triggered by a nearby companion. Nevertheless, fragmentation is not determined by the longest cooling times in the disk, but by the shortest. Nelson's disks did exhibit short cooling times at larger radii, in spite of this fact, did not fragment.

Rapid cooling of the disk midplane by convective-like motions in 3D disks has been shown to occur with several different codes (Boss 2004a, 2005; Boley et al. 2006; Mayer et al. 2006) and can lead to disk fragmentation (Boss 2004a, 2005), provided that the heat transported upward by these motions to the disk's surface can be radiated away to the protostellar envelope, a condition disputed by Rafikov (2006). The vertical structure model of Nelson (2000) assumed efficient vertical energy transport via convection, but did not produce fragmentation. The thermal boundary conditions on the disk surface then become of critical importance, and these boundary conditions are the subject of current research. Until the issue of disk thermal boundary conditions can be

further clarified, it is useful to ask whether for relatively short cooling times, comparable to or less than the orbital period, binarity promotes or suppresses fragmentation. The latter question is what both Mayer et al. (2005) and Boss (2006b) tried to answer.

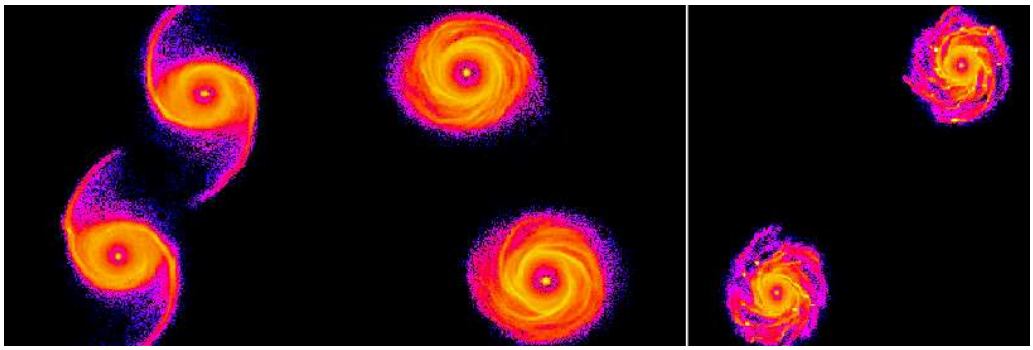

Fig. 6. Face-on density maps for two simulations of interacting $M = 0.1M_{\odot}$ protoplanetary disks in binaries with $t_{cool} = 0.5P_{rot}$ viewed face-on. The binary in the left panel has a nearly circular binary orbit with an initial separation of 60 AU and is shown after first pericentric passage at 150 yrs (left) and then at 450 yrs (right). Large tidally induced spiral arms are visible at 150 yrs. The right panel shows a snapshot at 160 yrs from a simulation starting from an initial orbital separation that is twice as large. In this case, fragmentation into permanent clumps occurs after a few disk orbital times. Figures adapted from *Mayer et al.* (2005).

Mayer et al. (2005) explored a range of cooling times, from less than 0.5 to 1.5 times the orbital period. They found that the effect of binarity changed with disk mass: except for the shortest cooling time ($0.3T_{orb}$), massive disks $M_{disk} = 0.1M_{\odot}$ that fragmented in isolation did not fragment when in a binary with a separation of ~ 60 AU, while disks with masses $0.05 - 0.08M_{\odot}$ that do not fragment in isolation do fragment in a binary system with a separation of ~ 60 AU provided that the cooing time is somewhat shorter than the disk orbital time. When the separation grows from 60 to 116 AU the behaviour of the disks becomes almost indistinguishable from that seen in isolation, and now fragmentation becomes possible in the $0.1M_{\odot}$ disks. Simulations from this work are presented in Figure 6, which shows how larger separations are more favourable to fragmentation in the case of massive disks. Mayer et al. interpreted the different behvaiour of disks having different masses as the product of different net cooling times at different mass scales. In more massive disks the spiral arms grow stronger as they are better amplified by self-gravity; as a result, shocks are more oblique and disk material acquires higher eccentricities, resulting in overall higher Mach numbers and stronger heating. For a given cooling time, the "net cooling", namely the ratio between cooling and heating, is higher for lighter disks. Below some mass, however, the self-

gravity is so low that spiral arms cannot grow enough to trigger fragmentation, no matter how strong is the perturbation of the companion and even if the cooling time is comparable to or shorter than the disk orbital time. Figure 3 shows the temperature evolution of the disk in some of the runs performed in Mayer et al. (2005). It shows that temperature increase in the outer disk, which opposes fragmentation, is larger in more massive disks and at smaller binary separation, supporting the interpetration of the authors concerning why fragmentation can be suppressed. The results of Mayer et al. (2005) are not in conflict with those of Nelson (2000) for runs that have similar orbital parameters and comparable disk masses, i.e. disk/star systems with mass ratios of 0.1 and separations of $50 - 60$ AU. It is true that in some of the latter runs disks fragment in Mayer et al. (2005) while they never fragment in Nelson (2000), but this discrepancy is seen only for the shortest cooling times ($0.3 - 0.5 T_{orb}$) used in Mayer et al. (2005), these being more than an order of magnitude shorter than the typical cooling times of Nelson (2000).

Boss (2006b) used his standard radiative transfer approach to handle the disk thermodynamics, i.e., diffusion approximation radiation transport, Rosseland mean dust opacities, and detailed equations of state for the gas pressure and specific internal energy. One model from Boss (2006b) was particularly similar to that of Nelson (2000): the binary companions had semimajor axes of 50 AU in both models, and an eccentricity of 0.3 in Nelson (2000) and 0.25 in Boss (2006b). The initial value of Toomre's Q was ~ 2 throughout most of the inner disk in Boss (2006b) and in Nelson (2000), implying that both disks were initially stable. While the total system mass was twice as high in Boss (2006b) as in Nelson (2000), the ratio of the disk mass to the protostar mass was the same in both models, ~ 0.1. In the case of Nelson (2000), the disk formed strong spiral arms but never fragmented. It heated up as a result of of viscous dissipation and partially also because of the spiral shocks, finally reaching a steady state characterized by a Toomre Q in the range of 4 to 5, i.e., quite stable to the growth of gravitational perturbations. (Figure 8). By comparison, in the Boss (2006b) model (see Figure 7)

the disk also formed strong spiral arms, but a self-gravitating clumps was able to form as well, with a mass of 4.7 M_{Jup}. When Boss (2006b) ran an identical model, except with the binary companion on a more eccentric orbit ($e = 0.5$), the clump that formed at a similar time to the one in Figure 5 (above) was not massive enough (only 0.68 M_{Jup}) to be self-gravitating, though later in the evolution self-gravitating clumps did form. These two models show that in the models of Boss (2006b), the ability of a binary companion to induce disk fragmentation depends strongly on the orbital parameters of the companion.

It is important to note, however, that while Nelson (2000) was able to follow the evolution of the disks through several periastron passages, and monitor the resultant disk heating, Boss (2006b) only followed a single periastron, largely because of the pile-up of disk mass at the outer edge of the disk, an obvious numerical artifact that greatly reduced the value of carrying

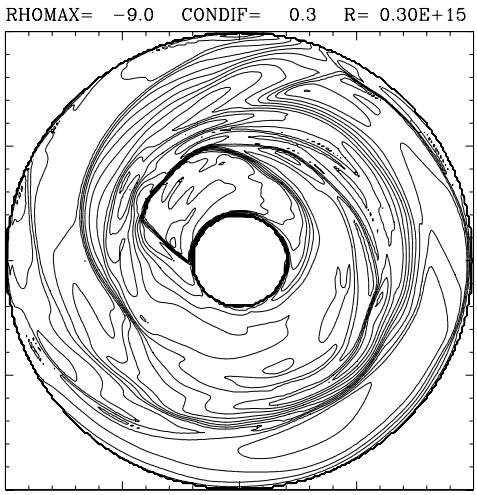

Fig. 7. Midplane density contours after 241 yr of evolution of a $0.091 M_{\odot}$ disk in orbit around a member of a binary $1 M_{\odot}$ protostar system, showing the formation of a self-gravitating clump of mass $4.7 M_{Jup}$ at 10 o'clock (Boss 2006b)

the models any further in time. Thus it is uncertain what would happen to the clumps that formed after the first periastron passage in the Boss (2006b) models, if subsequent periastron passages were calculated as well.

The models of Boss (2006b) investigated binary companions having eccentrcic orbits with semimajor axes of 50 or 100 AU, while those of Mayer et al. (2005) explored primarily 58 AU (13 models), as well as 4 models with $a = 116$ AU. The models with $a = 115$ AU fragment similarly to the 100 AU models in Boss (2006b). On the other end, for the models with $a = 58$ AU Mayer et al. (2005) found that whether or not fragmentation occurred depended on the disk masses and assumed cooling times, as described previously. The models with $a = 58$ AU separation, disk masses of 0.1 $M_{\odot}$ and protostars with masses of 1 $M_{\odot}$, can be compared directly with some of Boss's models having essentially the same parameters. While such models never fragment in Mayer et al. (2005) or produce transient clumps that disappear in a few disk orbital times, fragmentation always occurs in Boss (2006b). One subtletly in the comparison is that indeed even all the fragments obtained by Boss (2006b) are

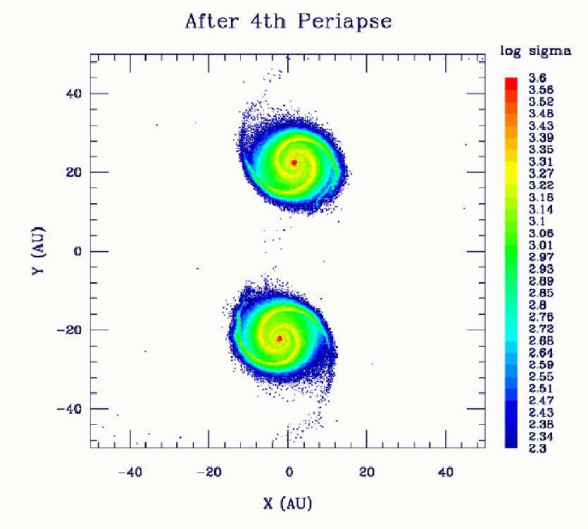

Fig. 8. Particle distribution of the binary system after periapse passage. Mass surface density units are in log (g cm^{-2}). The trajectory of each component is counterclockwise, and periapse occurs when the stars (at each disk center) reach the $y = 0$ axis and are 35 AU apart. The tidal torques have caused two-armed spiral structures to develop in the disks and significant mass redistribution, but no fragmentation. The figure has been adapted from Nelson (2000).

also transient fragments, because his finite-difference code is unable to provide the enhanced local spatial resolution that is needed to allow self-gravitating clumps to survive and orbit indefinitely. On the other end, Mayer et al. (2005) did not run the same model at higher resolution as they had done for isolated disk models in previous works (e.g. Mayer et al. 2004), and therefore one cannot exclude that their clumps would survive longer or fragmentation would be aided in the first place with an increased number of particles and proportionally smaller softening length. The azimuthal resolution in Boss (2006b) is indeed higher than that the hydrodynamical resolution and, even more, than the gravitational force resolution adopted by Mayer et al. (2005). In Mayer et al. (2005) mild overdensities build up along the spiral arms after periastron even in the runs that do not fragment (Figure 6), but are immediately dissolved; it is possible that with higher resolution they would become more nonlinear and collapse based on the preliminary results of the aforementioned code comparison between AMR and SPH codes (Mayer et al., in preparation). Nevertheless, the difference remains that a companion on a tighter orbit suppresses fragmentation according to Mayer et al. (2005), while it promotes it according to Boss (2006b). The intense heating is the reason of such suppression of fragmentation in Mayer et al. (2005), and such heating is apparently not present in Boss (2006b). Whether the SPH artificial viscosity is biasing

the results too much with the stronger shocks present in binary systems or whether the disks in Boss (2006b) cool too fast is at the moment unclear. It is especially noteworthy that Nelson (2000) studied a 50 AU binary system with SPH, at lower resolution than in the Mayer et al. work. This system should therefore be even more strongly affected by the presence of heating from artificial viscosity. In spite of this, Nelson finds that in fact the disks are *too cold*, compared to the observed L1551 IRS5 system–implying still more heating is required than artificial viscosity provides, making his disks even less likely to fragment.

Another difference in the setup that might explain the discrepancies is the fact that in Boss (2006b) the companion is simply a protostar, while it is a disk with a protostar in Mayer et al. (2005). In tighter binary systems the presence of the other disk might have an effect; indeed near periastron the two disks almost touch each other, possibly enhancing tidal and compressional heating on one another compared to the case in which only a companion star is present. Since the orbits in Mayer et al. (2005) are nearly circular, in the 58 AU case the two disks are almost always in the latter situation. This would also mean, however, that the behavior of real tight binary systems, which will normally have two disks orbiting each other, should be closer to what found by Mayer et al. (2005) and Nelson (2000).

4.2 Disk evolution: internal vs. external

The question also arises of how much of the disk restructuring is due to the disk's self-gravity and how much to tidal torques induced by the companion. Figure 9 shows the evolution of the disk surface density profile in one of the binary disks simulations of Mayer et al. (2005) evolved both with and without self-gravity. Clearly some mass transport has happened even without self-gravity. Such mass transport is the result of tidal torques induced by the gravitational interaction with the companion and the fact that little disk material exists in the initial state inside 4 AU to resist the flow of additional material inward. These tidal torques produce a two-armed spiral mode in the otherwise passive disk. The disk becomes truncated to a smaller radius and more mass piles up in the inner few AU as the arms redistribute angular momentum. We recall that the disks is Mayer et al. (2005) have been slowly grown in mass in isolation before being evolved with a companion; while the disk evolves in isolation the inner hole present in the initial conditions is gradually filled, and therefore the rapid accumulation of mass seen in the binary case is not an artificial result of the inner boundary condition. The mass inflow produces compressional heating, raising the temperature of the disk inside 10 AU. Exchange of mass between the two disks occurs but their mass varies by only $\sim 10\%$.

Despite the fact that the tidal interaction modifies the disk structure irrespective of disk self-gravity, Figure 9 shows that such changes are moderate compared to those occurring when self-gravity is included. When self-gravity

is included the density peak that develops is almost a factor of 2-3 higher than the maximum density in similar disk models evolved in isolation (Mayer et al. 2004). This statement applies to all of the runs in Mayer et al. (2005).

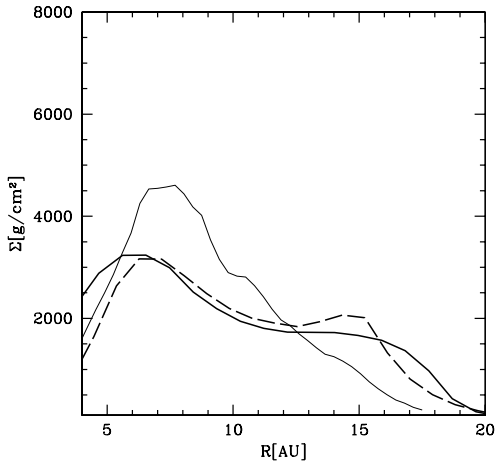

Fig. 9. Azimuthally averaged surface density profile of a disc with mass $M_d = 0.01M_\odot$ at $t = 0$ (solid line) and for its evolved state after being run without self-gravity for two orbits around an equally massive companion (dashed line). The surface density of a run employing a massive disk ($M = 0.1M_\odot$) evolved with self-gravity is shown instead by the thin solid line. A cooling time equivalent to 0.3 the orbital time was adopted in both runs. The figure has been adapted from Mayer et al. (2005).

The larger density may explain why models with masses lower than $0.1M_\odot$ become more prone to fragmentation when perturbed by a binary companion; evidently in these lighter disks the heating from shocks is not enough to compensate such a large density increase. Since disks are truncated within 15 AU, when clumps form they do so within such radius, typically between 8 and 12 AU. The locations where they form correspond to the location of the density maximum and are slightly closer to the star compared to those of clumps in the isolated disks studied by Mayer et al. (2004). In fact in isolation gravitationally unstable disks typically develop a density maximum between 12 and 15 AU, and that is where Q drops below 1 and fragmentation occurs (Mayer et al. 2004). The conclusion is that in all the simulations of Mayer et al. (2005) the restructuring of the disk results from a combination of tidal torques and self-gravity of the disks.

4.3 Temperatures in binary self-gravitating disks and effects on dust grains

Both Nelson (2000) and Mayer et al. (2005) found significant heating along spiral shocks in binary systems. Mayer et al. (2005) found that the temperatures can be a factor of 2-3 higher relative to the same disk in isolation for disks in the mass range $M_{disk} \sim 0.05 - 0.1 M_{\odot}$. This has important implications for the destruction of dust grains, hence on the formation of planetesimals, and thus of those Earth-sized rocky cores that are a necessary step to form giant planets in the core-accretion model. The consequence of the high temperatures in the GI active outer region of the disk is the vaporization of ice grains, which constitute as much as $30 - 40\%$ of the dust content in the disk. The actual surface density of solids might be reduced by up to 40% compared to isolated disks. The direct consequence should be that core accretion will be less efficient in binary systems compared to isolated disks. The results of Nelson (2000) are shown in Figure 10. Strong heating is instead absent in light disks ($M_{disk} 0.01 M_{\odot}$, whose temperatures increase by less than 50%. Therefore core accretion should be favored in such light disks, with masses comparable to the minimum mass solar nebula, because a larger relative dust content should be maintained. Those, however, are also the disks in which the growth of rocky cores of a few Earth masses (necessary to trigger runaway gas accretion) would take longer owing to their low surface densities.

A caveat in the above discussion is that the surface density of massive disks ($M > 0.05 M_{\odot}$at distances $10 - 15$ AU from the center is 50% higher than it would be without a companion by the end of the simulation. Assuming a uniform gas-to-dust ratio in the disk, the increase in surface density could compensate for the vaporization of dust grains, making massive disks not less favourable then light disks for giant planet formation via core accretion (see above). Spiral arms might also gather solids as a result of pressure gradients (Rice et al. 2004, 2006) leading to an enhanced gas-to-dust ratio inside them, another effect that could favour core accretion. Only more realistic calculations incorporating directly both vaporization and the dynamical dust particles within the gaseous disk will be able to settle this issue.

4.4 Effects of artificial viscosity

Boss (2006b) did not employ artificial viscosity in his standard models, but did turn on the artificial viscosity in a subset of models designed to determine to what extent the use of artificial viscosity in either a finite-difference code (e.g., Pickett et al. 2000) or an SPH code (e.g., Nelson 2000) might affect the disk instability process. Boss (2006b) ran four models with varying amounts of artificial viscosity, and found that only when the artificial viscosity was set to a value a factor of 10 times higher than the nominal value did the disk become so hot as to appreciably stifle fragmentation.

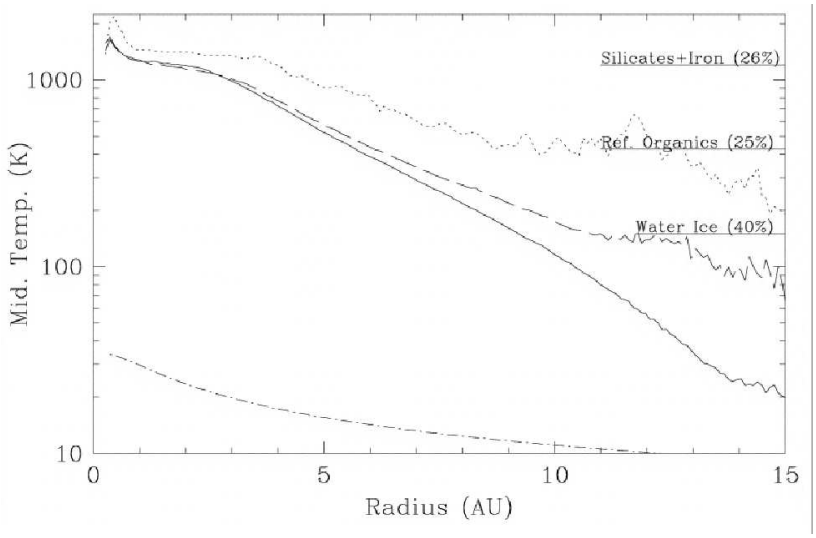

Fig. 10. Temperature profiles of the disks in Nelson (2000) shown before (solid line) and after (dashed line) the 4th periapse. The initial profile is shown with a dashed-dotted line. The dotted line shows the maximum temperature reached inside the spiral arms at that radius. At the right are vaporization temperatures of the major grain species in the solar nebule and their fraction of the total grain mas, as discussed in Pollack et al. (1994).

One possible source of the different outcomes between the results of Boss (2006b) and Nelson (2000) is the amount and effect of artificial viscosity assumed in the two sets of models. Artificial viscosity equivalent to an effective α viscosity with $\alpha = 0.002$ to 0.005 was intentionally included in the Nelson (2000) models in order to include the effects of shock heating. In the Boss (2006b) models, artificial viscosity was not used, but the level of implicit numerical viscosity appears to be equivalent to $\alpha \sim 10^{-4}$ (Boss 2004b), about 20 to 50 times lower than that in Nelson (2000). Given the experiments of Boss (2006b) with artificial viscosity, the use of this level of artificial viscosity in Nelson (2000) is consistent with the absence of fragmentation and the difference in cooling times in the two sets of models. Relatively short cooling times are obtained in models without artificial viscosity ($\sim$ 1 to 2 orbital periods, Boss 2004a), compared to the effective cooling time obtained in Nelson (2000) of $\sim$ 5 to $\sim$ 15 orbital periods, for orbital distances from 10 AU to 5 AU, respectively.

The use of artificial viscosity by Nelson (2000) was motivated by a good reason, namely to model shock dissipation in the disks, and produced substantial heating in the disks. Nevertheless, an analysis of the flux densities derived from his simulations fell nearly an order of magnitude short of that

required to reproduce the observations of the L1551 IRS5 binary system, on which his initial conditions were based.

It is of some interest that Boss & Yorke (1993, 1996) were able to match spectral energy distributions of the T Tauri system with axisymmetric disk models similar to those that form the basis for Boss (2006b) models, without using artificial viscosity. A part of the contradiction can perhaps be explained by the fact that the system modeled by Boss and Yorke was T Tau, a system at a much later evolutionary stage than L1551 IRS5, with correspondingly different energy output. We look to future observations using the ALMA telescope with great interest, because of the likelihood for observing younger, and much more deeply embedded objects, of greater relevance to the earliest stages of disk evolution where gravitational instabilities are more probable.

4.5 Initial conditions in the context of star formation

Are the initial conditions adopted in the existing simulations of binary, self-gravitating protoplanetary disks realistic? In reality, the two disks will be communicating since their beginnings, undergoing mass transfer and growing out of gas flowing from the periphery of the molecular cloud core. This is quite different from the setup assumed in the simulations. Tidal perturbations and mass transfer might be too sudden in the computations described in this chapter, while they will be achieved gradually in reality. However, if star formation occurs in gravoturbulent clouds, such as those modeled by Bate et al. (2002b), rather than in isolated cores, disks will not have time to slowly adjust to such an extremely dynamic environment by the time they become gravitationally unstable. First of all, one way binary systems can arise is via fragmentation of a bar-unstable core (Bate & Burkert 1997). This occurs on the orbital timescale of the rotating core , a few hundred years to 10^3 years, i.e. of the same order of the binary orbital time considered in all the three papers discussed here, rather than than on the collapse time of the cores, in the range 10^3 to 10^4 years. The collapse of the individual cores would occur on a timescale much smaller than the average collapse timescale of the larger star-forming region. A short collapse time of cores is suggested also by observations. Two examples are the observations that prestellar cores have large enhancements in column densities and that molecular abundances in them are consistent with a rapid collapse (Aikawa 2004). The resulting systems would have undergone several tidal interactions with bound or unbound companions since their birth. Turbulent molecular clouds have velocity dispersions of order $2-5$ kms^1, which means the typical crossing time of a region 10^{-2} pc in size will be $\sim 10^3$ years, The characteristic timescale of encounters between cores in such a turbulent cloud has to be of the same order of the latter timescale, i.e. once again comparable with the binary orbital time. Nevertheless, Mayer et al. (2005) studied the case of two self-gravitating disks reaching gradually the conditions present at the begining of the simulations by starting with very light, nearly non-self gravitating disks and growing the disk slowly over the

course of a few binary orbital periods (Figure 11). This way the disk profile has time to adjust. The spiral arms tidally induced on the third orbit are indeed slightly weaker than those in the standard run, and transient localized overdensities are apparent that were not present before, but no gravitationally bound clumps occur and the outer disk temperature after one orbit (~ 300 K) is comparable to that in the original run

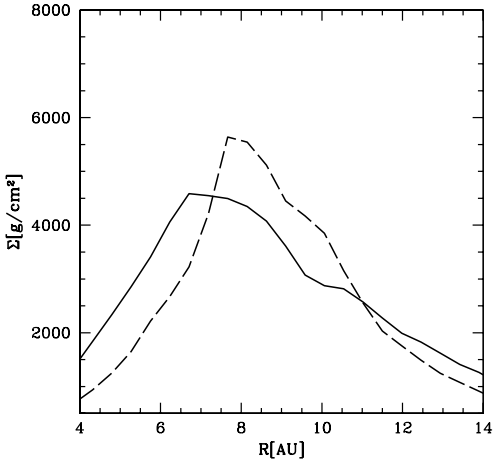

Fig. 11. Azimuthally averaged surface density profile after two binary orbits for a run employing two massive disks with $M = 0.1 M_{\odot}$. The disks were evolved with a cooling time equivalent to 0.3 the local orbital time with self-gravity (solid line) and with self-gravity switched off on the first binary orbit (dashed line).

The final surface density profiles of the disks in the two runs are also quite similar. Mass redistribution due to gravitational torques leads to a profile which cannot be described by a single power-law, has a remarkable density peak close to $7 - 8$ AU, and is steeper than r^{-2} outside this radius (Figure 9,11). The surface density profiles are steeper than those produced by gravitational instabilities when there is no companion. The mass inflow towards the center is greater. One would be tempted to conclude that the viscous evolution of the disk, where the "viscosity" is due to gravitational instability, is faster in binary systems. This might lead to a faster dissipation of the disk and a faster growth of the star since gas flows outside in. Some difficulty remains in establishing a solid connection because it is not clear how the large, initially massless hole in the middle of the disks, affects the mass transfer further out.

In the simulations of Mayer et al. (2005) the restructuring of the disk results from a combination of tidal torques and intrinsic self-gravity (see section 4.5). Since in the early stages protoplanetary disks should be massive enough

to be self-gravitating (Yorke & Bodenheimer 1999), it seems that this profound restructuring driven by the two simultaneous effects will likely occur in binary systems, and will occur early.

New SPH simulations with a variable equation of state (Bate 2001) that use a variable mass resolution technique to reach down to achieve a spatial resolution of $\sim 0.1AU$ in a rotating (non turbulent) collapsing molecular core of a fraction of a parsec in siz do indeed show substantial evolution of binary disks and mass inflow towards the central star just as a result of self-gravity. The rapidly rotating core collapses, becomes bar unstable and fragments into two clumps that later become a pair of pre-stellar cores surrounded by a fairly large, tidally truncated disk (about 30 or 80 AU in size), as shown in Figure 12. The two systems have unequal masses; while each system starts out with more than 2/3 of the mass being in the disk and the rest in a dense central clump, the precursor of the star, less than 0.1 AU in size, after about two binary orbits (corresponding to $\sim$ 2000 years and to the time at which we stopped the simulation) more than half of the disk mass has accreted onto the central clump. At this stage disks are slightly lighter than the central clump. Removal of angular momentum results from a combination of spiral instabilities in the disks and tidal torques from the companion, with te spiral arms being strengthened by the perturber as well. The physical driver of accretion is just gravity in these simulations since no other mechanisms to remove angular momentum are present except gravitational torques (both intrinsic and tidal). The only caveat is that artificial viscosity, while required to model physical dissipation in shocks correctly, might also enhance angular momentum transport. The accretion rate from the disk onto the central protostar at the end of the simulation is nearly $5 \times 10^{-}5 M_{\odot}/yr$, or about ten times higher than the accretion rate from the core onto the disk, for the lightest, and thus the most tidally perturbed, among the two systems, and about a factor of two lower for the other one.

5 Conclusions

We have noted that a number of numerical and physical effects can either encourage or discourage a disk instability from forming self-gravitating clumps that could become gas giant protoplanets. There are indications that the artificial viscosity used in SPH codes (Mayer et al. 2005, Nelson 2000) generally tends to suppress fragmentation (Mayer et al. 2004) although the simulations of Nelson (2000) had a lower artificial viscosity and yet did not find fragmentation. However, when artificial viscosity is such that simulations can match fluxes observed from protostellar systems, the resulting high level of disk heating can prevent fragmentation. Using a gravitational softening length that is smaller than the SPH smoothing length throughout most of the disk evolution, as in Mayer et al. (2005), favors fragmentation, as does the discreteness noise in SPH. Sharp disk edges promote fragmentation, while low resolution

(mass resolution in SPH, as set by the number of particles, or grid size in grid codes) seems to suppress fragmentation (Mayer et al. 2004; Boss 2000), but not always, as seen by Nelson (2006), where it enhanced fragmentation. The dependence on resolution is currently being investigated systematically in an on-going code comparison that involves both SPH and adaptive mesh refinement (AMR) codes; preliminary results confirm an increasing susceptibility towards fragmentation with increasing resolution (Mayer et al., in preparation). A prevalence of low order modes (Nelson 2000; Mayer et al. 2005; Boss 2006b) promotes fragmentation, as overdensities that occur on larger scales are easier to resolve with finite resolution. Finally, and perhaps most importantly, short cooling times promote fragmentation (Mayer et al. 2005), while long cooling times prevent it altogether (Nelson 2000).

Mayer et al. (2005) found that binary companions with semimajor axes of 58 AU prevented disk fragmentation, unless the disks had moderate masses ($0.05 - 0.08 M_{\odot}$) and cooled rapidly, indeed faster than even simulations that appeal to convective cooling suggest (Boss 2002, 2003; Mayer et al. 2006). They also found that when the semimajor axis was raised to 100 AU, fragmentation or transient clump formation resulted in all cases studied. The results for large separations are not in contrast with those of Boss (2006b). Instead, those for separations of 58 AU are in disagreement with Boss (2006b), who found fragmentation and transient clump formation even for semimajor axes of both 50 AU, although even closer encounters (i.e., higher eccentricities) tended to work against the formation of self-gravitating clumps. The results of Mayer et al. (2000) are not in contrast with those of Nelson (2000), although Nelson's disks were not fragmenting even in isolation according to Nelson et al. (2000), which does not allow to formulate the same conclusion reached by Mayer et al. (2005) , namely that fragmentation is generally suppressed in tight binary systems. Moreover, we note that most of the disks used by Mayer et al. (2005) were marginally unstable by construction ($Q < 2$), and therefore the fragmentation seen for larger semi-major axes might simply reflect the fact that as the separation increases the results tend to converge to those for disks with no binary companion. This in other words means that the fragmentation seen in such cases could have nothing to do with the tidal perturbation of a companion. Conversely, Boss uses mostly disks that would be stable in isolation ($Q \sim 2$ or larger), and hence the only logical outcome of his calculations in presence of a companion is either that the disk remain stable or that fragmentation is enhanced (i.e. no experiment was constructed to see whether fragmentation could be suppressed). This different logic behind the design of the simulations in the two works complicates the comparison and calls for future attempts by these and other authors to perform and compare exactly the same experiment.

The results of Mayer et al. (2005) and Boss (2006b) suggest that the formation of gas giant planets around binary stars with semimajor axes of 100 AU or larger may be possible by the disk instability mechanism. Note that for these systems core-accretion is in principle possible as well since spiral shocks

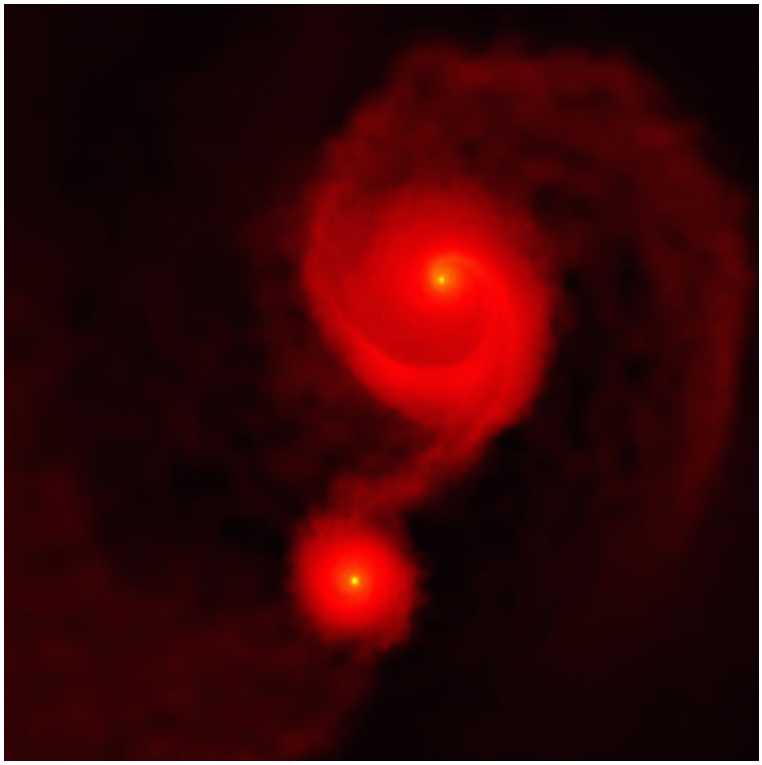

Fig. 12. Color coded density map of a binary protostar+disk system resulting from the collapse of a rotating molecular cloud core with initial density profile $\sim r^{-1}$. The box is 200 AU on a side, and the system is shown about 5×10^4 years after the collapse has been initiated, and a couple of binary orbits after the two disks have formed from the fragmentation of a bar-unstable, rapidly rotating protostellar core. The larger system weights $\sim 0.5 M_{\odot}$, while the smaller system weights only $\sim 0.15 M_{\odot}$. The total mass of the molecular core was $1 M_{\odot}$ and its size 10.000 AU at t=0. The simulation employs 500.000 particles in total, but the mass resolution in the inner 500 AU is higher than in the surrounding volume, so that as many as 4/5 of the particles are used only in this inner region

do not heat the gas to temperatures high enough to vaporize major dust grain species (Mayer et al. 2005). For smaller semimajor axes the situation is much more complex. For the latter, Mayer et al. (2005) conclude that disk instability is unlikely but that core-accretion might happen once the disk is light enough, $M \sim 0.01 M_{\odot}$ (e.g. as a result of accretion onto the star) that it can only form weak spiral shocks in which grains easily survive. This is because in Mayer et al. (2005) the role of self-gravity, and thus of disk mass, in the determining the strength of the spiral shocks is crucial (see above). Nelson (2000) claimed that both disk instability and core-accretion would be unlikely in such systems, drawing the same conclusion that Mayer et al. (2005) would

have reached had they not considered binary systems composed of light disks (but see above section 4.3 for possible caveats). Finally, Boss (2006b) finds that these systems would fragment, although he cannot follow the clumps for a long enough time to show that they are long lasting. Despite the fact that disagreements exist between the different works, it is clear from now that the tightest binary systems might become an ideal testbed for theories of planet formation. It is thus important for observers to refine their estimates of the semimajor axes of binary systems containing gas giant planets, in order to learn if these systems could have been formed by disk instability. Post-formational orbital evolution of multiple systems (e.g., decay of an unstable triple system) might be another means to explain the observed binary systems with gas giant companions. Finally, we recall that for intermediate semi-major axes orbital eccentricities might also be important. Indeed, while Mayer et al. (2005) adopt nearly circular orbits, Boss (2006b) chooses eccentric orbits. Hence in Boss (2006b), for a given semi-major axis, the disks will spend a larger fraction of the orbital time far away from each other. The tidal perturbation will be more impulsive rather than contiunous. In other fields of astrophysics which deal with similar problems, such as in the study of galaxy interactions, it is well known that impulsive or continuous tidal heating give rise to quite different responses in a self-gravitating system, to the point of determining a completely different structural evolution (Mayer et al. 2001). What is seen in particular in the case of galaxies is that impulsive encounters can generate "cold" features such as bars that then survive for many orbital times, but the same features are erased as the object increases too much its kinetic energy and/or thermal energy owing to a continuous tidal perturbation such as that associated with circular or nearly circular orbits. Similarly, one could speculate that in encounters between disks on eccentric orbits transient overdensities might have a better chance to survive as the same tidal force that triggered their formation fades away later towards the apocenter of the the orbit. Again, simulations exploring a larger parameter space are needed to assess if eccentricity is such an important parameter and might help to partially reconcile the disagreement between Boss (2006b) and Mayer et al. (2005). Disks perturbed by fast-fly bies of other stars or brown dwarfs also suffer significant tidal heating and do not fragment unless the cooling time is very short (Lodato et al. 2007).

A major source of the differences obtained by Nelson (2000) and Mayer et al. (2005) relative to Boss (2006b) could be the use of artificial viscosity in the first two works based on SPH and its neglect by Boss (2006b) The much longer cooling times in Nelson (2000) are also expected to stifle fragmentation. Clearly, when artificial viscosity is used to heat a disk, and this heat is unable to escape on an orbital time scale, the chances for clump formation by disk instability are severely reduced. This is a general issue for the disk instability model, irrespective of the presence or not of a binary companion. Some of the heating associated with artificial viscosity will indeed a rise in nature as a result of turbulence and other unresolved aspects of hydrodynamical

flows. It remains for future work to determine what is the proper amount of artificial viscosity to be used in simulating realistic protoplanetary disks, and to determine the proper boundary conditions at the surfaces of protoplanetary disk that will allow the disk to radiate away energy at the correct rate. The sensitivity to the cooling time is readily shown by the first in a series of new simulations of binary disks with the algorithm for radiative transfer described in Mayer et al. (2006). Intermediate mass disks $0.05 M_{\odot}$ that were fragmenting in binaries in Mayer et al. (2005), this being the only for which fragmentation was found even for orbits with separations of 58 AU at sufficiently short cooling times, develop strong spiral arms but no clumps when flux-limited diffusion plus atmospheric cooling via blackbody radiation is used (see Figure 13). This is not surprising since this latest radiation physics model yields cooling times of order or slightly longer than the orbital time (apparently via convection) while in Mayer et al. (2005) these disks were fragmenting with shorter cooling times, half or less than half the local orbital time. Indeed the average outer disk temperatures (outside 5 AU) in these new simulation is larger than 100 K, in comparison with $60 - 70$ K in the corresponding run of Mayer et al. (2005). The results of this simulation are in good agreement with those of Nelson (2000).

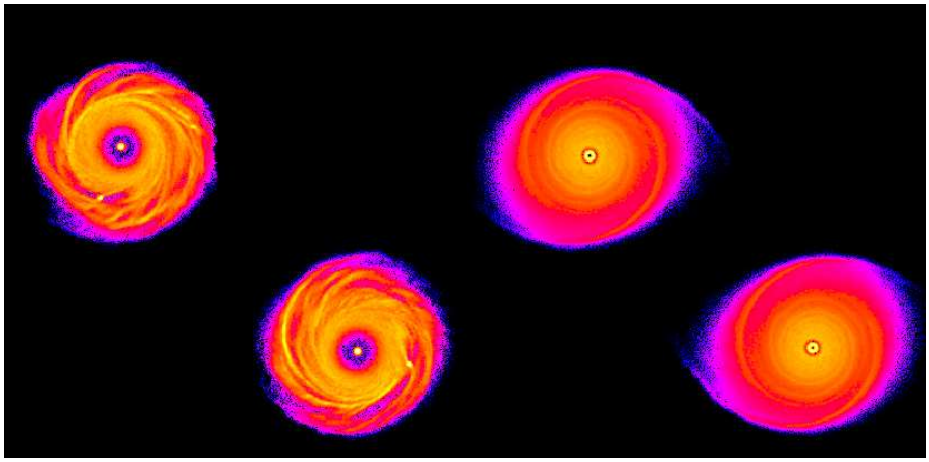

Fig. 13. Color coded density maps of two runs employing two disks with masses $0.05 M_{\odot}$ moving on a binary orbit with average separation of 60 AU. The results are shown after 1.5 binary orbits. On the left a run in which the cooling time is fixed to 0.3 orbital time is shown, on the right a newer run in which flux-limited diffusion is employed and the disk cools at the surface as a blackbody, resulting in a cooling time slightly longer than the orbital time. Clump formation has occurred in the run with the short cooling time while the in other run the two disks have achieved a higher temperature, lower densities and a much weaker spiral structure.

However, the observational fact that binary stars with separations small enough for mutual tidal interactions to be important are orbited by gas giant planets means that somehow these planets can indeed form even in these systems. Given the problems that core accretion encounters as well in binary systems (Thébault et al. 2004), disk instability would seem to remain a possible means for forming gas giants in binary systems.

6 References

Aikawa, Y., Proceedings of the Conference "Star Formation at High Angular Resolution", International Astronomical Union Symposium 221, XXV General Assembly of the IAU, Sydney, Australia, 22-25 July 2003. Eds: M. Burton, R. Jayawardhana, T. Bourke, 67, 2004

Alexander, ??? & Ferguson, ??? 1994 ????

Bate, M. R. 2000, MNRAS, 314, 33

Bate, M. R. & Burkert, A. 1997, MNRAS, 228, 1060

Benz, W. 1990, in The Numerical Modeling of Stellar Pulsation, ed. J. R. Buchler (Dordrecht: Kluwer), 269

Benz, W. 1991 ???

Benz, W. et al. 1990 ???

Boley, A. C. et al. 2006, ApJ, 651, 517

Boss, A. P. 1993, ApJ, 417, 351

Boss, A. P. 1996, ApJ, 469, 906

Boss, A. P. 1997, Science, 276, 1836

Boss, A. P. 1998, ApJ, 503, 923

Boss, A. P. 2000, ApJ, 545, L61

Boss, A. P. 2001, ApJ, 563, 367

Boss, A. P. 2002, ApJ, 576, 462

Boss, A. P. 2003, ApJ, 599, 577

Boss, A. P. 2004a, ApJ, 610, 456

Boss, A. P. 2004b, ApJ, 616, 1265

Boss, A. P. 2005, ApJ, 629, 535

Boss, A. P. 2006a, ApJ, 637, L137

Boss, A. P. 2006b, ApJ, 641, 1148

Boss, A. P. & Myhill, E. A. 1992, ApJS, 83, 311

Boss, A. P. & Yorke, H. W. 1993, ApJ, 411, L99

Boss, A. P. & Yorke, H. W. 1996, ApJ, 469, 366

Cai, K. et al. 2006a, ApJ, 636, L149

Cai, K. et al. 2006b, ApJ, 624, L173 (Erratum)

Cameron, A. G. W. 1978, Moon Planets, 18, 5

Chauvin, G. et al. 2006, A&A, 456, 1165

D'Alessio, P., Calvet, N., & Hartmann, L., 2001, ApJ, 553, 321

Duquennoy, A. & Mayor, M. 1991, A&A, 248, 485

Durisen, R. H., Cai, K., Mejía, A. C. & Pickett, M. K. 2005, Icarus, 173, 417

Durisen, R. H., et al. 2007, in Protostars & Planets V, ed. B. Reipurth (Tucson: Univ. Arizona Press), in press

Eggenberger, A., Udry, S. & Mayor, M. 2004, A&A, 417, 353

Evrard, A.E. 1990, ApJ, 363, 349

Gammie, C. F. 2001, ApJ, 553, 174

Gingold, R. A. & Monaghan, J. J. 1977, MNRAS, 181, 375

Goldreich. P. & Lynden-Bell, D. 1965, ???

Herant, M. & Woosley, S. 1994, ApJ, 425, 814

Johnson, B. & Gammie, C. F. 2003, 597, 131

Kawakita, H., et al. 2001, Science, 294, 1089

Kuiper, G. P. 1951, Proc. Nat. Acad. Sci., 37, 1

Laughlin, G., Korchagin, V. & Adams, F. C. 1997, ApJ, 477, 410

Lin, D. N. C. & Pringle, J. E. 1987, MNRAS, 225, 607

Lodato, G. & Rice, W. K. M. 2004, MNRAS, 351, 630

Lodato, G., Meru, F. Clarke, C. & Rice, W. K. M. 2007, MNRAS, in press

Lucy, L. B. 1976 ???

Mayer, L., Colpi, M., Governato, F., Moore, B., Quinn, T., Stadel, J., & Lake, G., 2001, ApJ, 559, 754

Mayer, L., Quinn, T., Wadsley, J. & Stadel, J. 2002, Science, 298, 1756

Mayer, L., Quinn, T., Wadsley, J. & Stadel, J. 2004, ApJ, 609, 1045

Mayer, L., Wadsley, J., Quinn, T. & Stadel, J. 2005, MNRAS, 363, 641

Mayer, L., Lufkin, G., Quinn, T. & Wadsley, J., 2007, ApJ, submitted

Mejía, A. C., Durisen, R. H., Pickett, M. K. & Cai, K., 2005, ApJ, 619, 1098

Monaghan, J. J. 1992, ARAA, 30, 543

Morris, J. P., Monaghan, J. J., 1997, J. Comp. Phys., 136, 41

Nelson, A. F. 2000, ApJ, 537, L65

Nelson, A. F. 2006, MNRAS, 373, 1039-1073

Nelson, A. F., Benz, W., Adams, F. C. & Arnett, W. D. 1998, ApJ, 502, 342

Nelson, A. F., Benz, W. & Ruzmaikina, T. V. 2000, ApJ, 529, 357

Paczyński, B. 1978, ???

Papaloizou, J. C. & Savonije, G. J. 1991, MNRAS, 248, 353

Patience, J., et al. 2002, ApJ, 581, 654

Pickett, B. K., Durisen, R. H. & Davis, G. A. 1996, ApJ, 458, 714

Pickett, B. K., Durisen, R. H. & Link, R. 1997, Icarus, 126, 243

Pickett, B. K., Cassen, P., Durisen, R. H. & Link, R. 1998, ApJ, 504, 468

Pickett, B. K., et al. 2000, ApJ, 529, 1034

Pickett, B. K., et al. 2003, ApJ, 590, 1060

Pollack, J. B., McKay, C. & Christofferson, B. M., 1985, Icarus, 64, 471

Pollack, J.B., Hollenbach, D., Beckwith, S., Simonelli, D.P., Roush, T. & Fong, W. 1994, ApJ, 421, 615

Rafikov, R. R. 2006, ApJ, submitted (astro-ph/0609549)

Raghavan, D. et al. 2006, ApJ, 646, 523

Rice, W. K. M., Armitage, P. J., Bate, M. R. & Bonnell, I. A. 2003a, MNRAS, 339, 1025

Rice, W. K. M. et al. 2003b, MNRAS, 346, L36

Springel, V. & Hernquist, L. 2002, MNRAS, 333, 649

Thébault, P., et al. 2004, A&A, 427, 1097

Tomley, L., Cassen, P. & Steiman-Cameron, T. 1991, ApJ, 382, 530

Tomley, L., Steiman-Cameron, T. Y. & Cassen, P. 1994, ApJ, 422, 850

Toomre, A. 1964, ApJ, 139, 1217

Udry, S. Eggenberger, A., Beuzit, J.L., Lagrange, A.M., Mayor, M., & Chauvin, G., 2004, in "The Environment and Evolution of Double and Multiple Stars", Proceedings of IAU Colloquium 191, held 3-7 February, 2002 in Merida, Yucatan, Mexico. Edited by Christine Allen & Colin Scarfe. Revista Mexicana de Astronomi'a y Astrofi'sica (Serie de Conferencias) Vol. 21, pp. 215-216 (2004)

Wadsley, J., Stadel, J., & Quinn, T.R., New Astronomy, 9, 137

Yorke, H. W. & Bodenheimer, P. 1999, ???